A coherent feed forward loop drives vascular regeneration in damaged aerial organs growing in normal developmental-context

Dhanya Radhakrishnan,[1,†] Anju Pallipurath Shanmukhan,[1,†] Abdul Kareem,[1,†] Mohammed Aiyaz,[1,†] Vijina Varapparambathu,[1] Ashna Toms,[1] Merijn Kerstens,[2] Devisree Valsakumar,[1] Amit N. Landge,[1] Anil Shaji,[1] M. K. Mathew,[1,3] Megan G.Sawchuk,[4] Enrico Scarpella,[4] Beth A.Krizek,[5] Idan Efroni,[6] Ari Pekka Mähönen,[7,8] Viola Willemsen,[2] Ben Scheres,[2] and Kalika Prasad[1,*]

[1]School of Biology, Indian Institute of Science Education and Research, Thiruvananthapuram, 695551 India.

[2]Department of Molecular Genetics, University of Utrecht, Padualaan 8, Utrecht 3584 CH, The Netherlands Plant Developmental Biology, Wageningen University Research, Wageningen 6708 PB, The Netherlands.

[3]National Centre for Biological Sciences, Tata Institute of Fundamental Research, 15 Bengaluru,560065, India.

[4]Department of Biological Sciences, University of Alberta, Edmonton, Alberta, Canada

[5]Department of Biological Sciences, University of South Carolina, Columbia, SC 29208, USA

[6]The Robert H. Smith Institute of Plant Sciences and Genetics in Agriculture, The Hebrew University, Rehovot 76100, Israel.

[7]Institute of Biotechnology, University of Helsinki, 00014 Helsinki, Finland.

[8]Department of Biosciences, Viikki Plant, Science Centre, University of Helsinki, 00014 Helsinki, Finland.

†These authors contributed equally to the work

*Correspondence: kalika@iisertvm.ac.in

KEYWORDS: vascular regeneration; PLT; CUC2; wound repair; auxin; PIN1

SUMMARY STATEMENT

Plants constantly encounter adverse conditions capable of inflicting injuries. Our studies discover a coherent feedforward loop driven local auxin biosynthesis, as a key regulatory mechanism of vascular regeneration in damaged aerial organs of plants.

ABSTRACT

Aerial organs of plants being highly prone to local injuries, require tissue restoration to ensure their survival. However, knowledge of the underlying mechanism is sparse. In this study, we mimicked natural injuries in growing leaf and stem to study the reunion between mechanically disconnected tissues. We show that *PLETHORA*(*PLT*)/ *AINTEGUMENTA*(*ANT*) genes, which encodes stem cell promoting factors, are activated and contribute to vascular regeneration in response to these injuries. PLT proteins bind to and activate the CUC2 promoter. Both PLT and CUC2 regulate the transcription of the local auxin biosynthesis gene YUC4 in a coherent feed forward loop, and this process is necessary to drive vascular regeneration. In the absence of this PLT mediated regeneration response, leaf ground tissue cells can neither acquire early vascular identity marker ATHB8, nor properly polarize auxin transporters to specify new venation paths. The PLT-CUC2 module is required for vascular regeneration, but is dispensable for midvein formation in leaf. We reveal the mechanisms of vascular regeneration in plants and distinguishes the wound repair ability of the tissue from its formation during normal development.

INTRODUCTION

Plants are prone to numerous injuries in their lifespan, due to their sessile lifestyle. They are subjected to injuries caused by biotic factors such as pathogen attack and herbivory. Abiotic factors such as damaging weather conditions can also cause tissue damage. Unhealed wounds can compromise the plant fitness and survival, and tissue healing mechanisms have evolved to counteract the damage. Following wounding, regenerative responses may be restricted to local healing in the form of cell proliferation or may entail complete regeneration of damaged tissue or organ (Ikeuchi et al., 2016; Galliot et al., 2017). The capacity of plants to regenerate the complete body plan *in vitro* from excised tissue is a powerful demonstration of the versatility of plant regeneration processes and forms the basis for many horticultural applications (Kareem et al., 2015; Ikeuchi et al., 2016; Radhakrishnan et al., 2018).

In stem, cellular, molecular and hormonal interactions at wound sites coordinate wound healing and restore vasculature (Flaishman et al., 2003; Asahina et al., 2011; Pitaksaringkarn et al., 2014; Melnyk et al., 2015; Mazur et al., 2016). Auxin is important for vascular tissue regeneration in multiple plant species (Sachs, 1968, 1969, 1981, 1991). The canalization models that underlie this regeneration process rely on the potential of auxin to induce correctly polarized auxin transporters together with activation of vascular cell fate determinants (Wenzel et al., 2007; Donner et al., 2009; Ohashi-Ito et al., 2013). In the growing tips of shoots and roots, damaged meristematic cells are replaced using positional cues from neighbouring cells (van den Berg et al., 1995; Reinhardt et al., 2003).

In roots, regeneration involves reactivation of embryo-specific genes, proper reallocation of root cell-fate determinants and integration of auxin, cytokinin and jasmonate signals (Xu et al., 2006; Efroni et al., 2016; Marhava et al., 2019; Zhou et al., 2019).

Laser ablation and root tip resection studies have shown that stem cell activation is a vital step for regeneration of lost cells and entire organ (van den Berg et al., 1995; Xu et al., 2006; Marhava et al., 2019; Zhou et al., 2019). The stem cell regulators PLETHORA1 (PLT1) and PLT2 are essential for the re-establishment of quiescent centre (QC) cells upon laser ablation and for the regeneration of primary and lateral root tip following resection (Xu et al., 2006; Durgaprasad et al., 2019). *PLT1* and *PLT2* are induced by PLT3, PLT5 and PLT7 activity to regulate stem cell activation during lateral root development (Du and Scheres, 2017). In the shoot, members of *PLT* family along with AINTEGUMENTA (ANT) transcription factor

regulate the development and phyllotaxis of aerial organs (Prasad et al., 2011; Krizek, 2015). PLT factors also regulate hormone mediated *de novo* shoot regeneration (Kareem et al., 2015).

While several studies have addressed specific regeneration processes in specific plant parts or in excised organs and have the implicated factors regulating these processes, our knowledge of underlying molecular mechanisms of wound repair in aerial organs is limited (Ikeuchi et al., 2018). It is largely unknown how wound repair in leaf tissue relates to the normal developmental program. Here, we investigate vascular reprogramming after leaf damage from the viewpoint that tissue reprogramming may require stem cell factors identified in other regeneration contexts. We reveal an essential role of members of the *PLETHORA (PLT)/ AINTEGUMENTA (ANT)* gene family in activating regeneration responses. *PLT* genes act through *CUP-SHAPED COTYLEDON2* (*CUC2)* to repair wounds and regenerate vascular tissue in damaged aerial organs. Furthermore, we show that the *PLT-CUC2* module acts through local auxin biosynthesis, and is required for proper repolarisation of PIN auxin efflux facilitators and reprogramming of vascular identity in aerial organs. The *PLT-CUC2* module is strictly required for regeneration of leaf vasculature, but is not critical for the normal development of closed vein loops in the absence of perturbations.

RESULTS

PLT3, PLT5 and *PLT7* genes respond dynamically to mechanical injuries

PLT3, *PLT5* and *PLT7* collectively regulate tissue-culture-mediated *in vitro* shoot regeneration and will from here on be referred to as *PLT3,5,7*. *PLT3,5,7* regulated root stem cell regulators establish pluripotency in callus and *PLT3,5,7* regulated shoot promoting factors act in response to external hormonal cues to induce regeneration of the complete plant body (Kareem et al., 2015).

Interestingly, *PLT3,5,7* genes are expressed in the shoot during development and the positioning of aerial organs (Prasad et al., 2011; Krizek, 2015). To assess whether PLT3,5,7 function is required for repairing damaged inflorescence and leaf tissue without external hormonal cues, we determined whether expression of these genes is induced as a natural response to injuries that growing plants are likely to encounter such as local abrasions in the stem, partial stem incisions and midvein injuries in the leaf blade. These injuries were made without detaching any organ. After local abrasion that damaged epidermal and sub-epidermal layers including vascular tissue in inflorescence (Fig. 1A,A', Fig. S1A-D), *PLT7::PLT7-vYFP*

was induced 12 h post injury, prior to any apparent regeneration response (Fig. 1B,B'). The expression peaked at 36 h (Fig. 1C,C', Fig. S1F,F'). In response to partial incision of the inflorescence stem (Fig. 1D,D'), *PLT7::PLT7-vYFP* expression was upregulated at both ends of the incised stem, with relatively higher expression in the upper end after 6h (Fig. 1E,E'). The high level of expression continued for 12 h (Fig. 1F,F'). At 12 h, upregulated expression expanded beyond the partial slit, and at 24 h, it became confined to a narrower domain in the vicinity of the incision (Fig. 1F,F',G,G'). Transcript levels of *PLT7* were consistent with the fusion protein expression data and remained upregulated till 24 h (Fig. S1E). Similarly, when the midvein of a growing leaf blade was wounded, cells in the vicinity displayed pronounced upregulation of *PLT7::PLT7-vYFP* 12 h post injury (Fig. 1H,I). In response to injury, *PLT3::PLT3-vYFP* and *PLT5::PLT5-vYFP* also showed upregulation of expression in the vicinity of the wound albeit with some differences in the timing of their activation and in spatial distribution (Fig. 1J,K, Figs S1G-P',S2,S3). In response to leaf incision, while both PLT3 and PLT7 are expressed in close proximity to the wound, PLT5 is expressed predominantly in the vascular tissue near the damage (Fig. 1H-K, Fig. S3A,B)

Root stem cell regulators *PLT1*, *PLT2* and *WOX5*, which are activated by PLT3,5,7 during tissue-culture-mediated *in vitro* shoot regeneration (Kareem et al., 2015), did not reveal any expression in growing leaves and stems in response to injuries (Fig. S4).

PLT is required to activate innate regenerative responses to injuries in aerial organs

Aerial organs of growing plants are subject to substantial wear and tear and *PLT3,5,7* expression is rapidly activated in response to injuries (Fig. 1, Figs S1-S3). We therefore asked whether *PLT3,5,7* genes are required for wound repair and tissue regeneration in stem and leaf growing in the normal developmental-context of *Arabidopsis*.

Wound repair and vascular regeneration in inflorescence

We mimicked physical abrasion by damaging epidermis, sub-epidermal layers and vascular tissue locally (see the methods for details, Fig. 2A,A') in a growing inflorescence stem of wildtype as well as *plt3;plt5-2;plt7* mutant plants. In the wildtype, we noticed a healing response in the form of a visible mass of proliferating cells (callus-like growth) throughout the wound at 2 daa (days after abrasion), which became more prominent at 4 daa (Fig. 2B, Fig. S5A,B). Later, callus-like growth completely covered and sealed the wound. The inflorescence stems regained its growth following the repair process. In contrast to wildtype, the healing

response was severely reduced in injured *plt3;plt5-2;plt7* inflorescences and the wound sealing process was not completed in the triple mutant inflorescence (Fig. 2A',B', Fig. S5A',B'). Importantly the inflorescence stem development of uninjured mutant is comparable to wildtype (Fig. S5I,J).

Next, we made a partial slit in the inflorescence stem of wildtype and *plt3;plt5-2;plt7* mutant disrupting both vascular connections and ground tissue (Fig. 2C,C',E,E'). 24 h after the incision, wounded parts adhered in the wildtype inflorescence stem (Fig. S5C,D). Subsequently, cell proliferation was observed as indicated by visibly swollen tissues at cut ends followed by regeneration of vascular tissues at 4 dac (days after cut) (Fig. 2D,F). Subsequent restoration of growth and physiological functions were demonstrated by the development of new flowers and siliques (Fig. S5E). In contrast to wildtype, where the wound was healed on the 4th day, the *plt3;plt5-2;plt7* triple mutant displayed severely reduced callus-like growth at the wound site and ~49% inflorescence stems failed to regenerate vascular tissue (Fig. 2C'-F',G). Our data show the role of *PLT3,5,7* in activating a healing response in the form of callus-like growth and vascular regeneration to restore the damaged tissue in growing inflorescence stem.

Vascular regeneration in a growing leaf

Restoration of vasculature is a long-known feature of stem regeneration, and we investigated whether this response also occurred in leaves. We made a local injury in the midvein of a growing young wildtype leaf of a 5 dpg (days post germination) plant (for details refer methods section). To keep the developmental stage uniform, we injured the first pair of young leaves which displayed midvein formation but not lateral veins at the time of injury (Fig. 2H,H', Fig. S6A,A'). The injuries either (i) damaged the midvein without making an opening or (ii) completely disconnected the midvein leaving a gap between the vascular strands. In both the cases, cells in the vicinity of the midvein experienced mechanical perturbations due to the pressure applied by the needle. 4 days post injury (dpi), wildtype leaves repaired both types of injuries. In case (i), where the break was incomplete, the injured midvein was repaired and new vascular cells regenerated to restore the physiological connection (Fig. S6E). In case (ii), where there was a complete disconnection, we observed regeneration of vascular strand either connecting together the cut ends of the midrib or connecting the cut end of midrib to a lateral vein (Fig. 2I,J). Strikingly, after local injury in the midvein of young wildtype leaf blades, ~80% of the samples regenerated vascular tissue in response to incision (Fig. 2L). The

regenerating vascular cells often bypassed the damaged area and reunited with the lower half of the midvein making a D-shaped loop around the wound site similar to Sachs' observation of vascular regeneration around the wound site in the epicotyl stem of pea plant (Sachs, 1981) (Fig. 2I). Alternatively, they formed a new connection to the nearest lateral vein (Fig. 2J). The non-regenerating lower vascular strand degenerated after residual proliferation at the cut end (Figs S5L,S6B). We followed vascular regeneration from the time of injury to distinguish between the vascular strand reuniting the midvein regenerating from the cut end as opposed to recruiting a pre-existing lateral vein developed during leaf growth (Fig. S6A-D'). When the injury left a wider hole in the leaf blade exceeding 400 microns between the cut ends of the midvein, we rarely observed any vascular regeneration (Figs S6F-I,S7A). Such injuries left behind only an unorganised mass of cells (Fig. S6H). We therefore restricted our subsequent analysis to leaf blade injuries that completely disconnected the midvein leaving a gap well under 400 microns between the cut ends.

In contrast to wildtype leaves where ~80% of the injured leaves regenerated vascular strands, only ~40% of injured *plt3;plt5-2;plt7* leaves could regenerate and the rest completely failed to regenerate vascular strands (Fig. 2H',I',L). In non-regenerating mutant leaves, lateral veins failed to connect to the midvein near the wound site (Fig. 2I'), but an unorganised mass of proliferating cells at the wound site were observed, mostly at the cut ends of upper vascular strands and on the epidermis (Fig. S7B-D). Many such leaves displayed poor growth and failed to develop properly (Fig. S7E). It is important to note that uninjured *plt3;plt5-2;plt7* mutant plants did not display any defects in the formation of closed vein loops (consisting of midvein and secondary veins) as compared to wildtype but were severely impaired in vascular regeneration (Fig. 2L, Fig. S7F-I). With respect to leaf morphology, we did not observe any defects in the first pair of leaves (Fig. S5F,G). Among double mutant combinations, while 70% of *plt3;plt5-2* and *plt5-2;plt7* double mutants regenerated vascular stands in response to injury, only ~64% of *plt3;plt7* double mutant leaves regenerated vascular tissue (Fig. S8A).

The closely related *AINTEGUMENTA (ANT)* gene marks stem cells of root vascular cambium and acts redundantly with *PLT3* and *PLT7* during plant development (Krizek, 2015; Smetana et al., 2019). *ANT* is strongly expressed in the vascular tissue of young leaves (Fig. S8B). We therefore examined vascular regeneration in *plt3;plt7;ant4* triple mutant plants in response to midvein injury. Strikingly, none of the tested *plt3;plt7;ant4* seedlings regenerated vascular tissues demonstrating an essential role of *ANT* with *PLT3* and *PLT7* in vascular regeneration

(Fig. 2K,L, Fig. S8C). Because of the severity of shoot phenotypes in *plt3;plt7;ant4* (produces only leaves but no stem) we chose the *plt3;plt5-2;plt7* mutant, which developed normal leaves as well as an inflorescence comparable to wildtype, to probe the mechanism of vascular regeneration using further assays (Prasad et al., 2011; Krizek, 2015). Taken together, our data reveal a previously unrecognised role of *PLT3,5,7* and *ANT* in repairing damaged tissues during plant growth.

***PLT5* and *PLT7* are sufficient for promoting vascular regeneration and wound repair**

Tissue/organ regeneration is closely linked to cellular reprogramming. We next asked whether *PLT* genes are sufficient to activate cellular reprogramming leading to enhancement of wound repair. Strikingly, inducible overexpression of PLT5 (*35S::PLT5-GR*) or PLT7 (*35S::PLT7-GR*) promoted multiple strand formation from the regenerating midvein in response to injury (Fig. 3A,A',C,C', Fig. S8D). Similarly, inducible overexpression of PLT5 or PLT7 enhanced wound repair at the cut ends of detached organ and in response to inflorescence abrasion (Fig. 3B,B',D,D', Fig. S8E-F'). Consistent with the ability of PLT to promote cell division upon wounding, transcripts of *CYCLIN* genes increased in growing seedlings upon inducible overexpression of PLT5 (*35S::PLT5-GR*) (Fig. S8G). These results suggest that PLT are sufficient to promote wound repair and multiple vascular strand regeneration in response to injury.

We addressed whether PLT-like proteins from other plant species can trigger regeneration. Rice is a morphologically diversified monocot plant, while *Arabidopsis* is a dicot. Expression of rice *PLT*-like gene O*sPLT2* under the *Arabidopsis PLT5* promoter in a *plt3;plt5-2;plt7* mutant (*plt3;plt5-2;plt7;AtPLT5::OsPLT2-vYFP*) healed damaged *Arabidopsis plt* mutant inflorescence by inducing cell proliferation as evident from upregulated expression of cell cycle progression markers (Fig. 3E-G, Fig. S8H,I). Furthermore, *OsPLT2-vYFP* rescued leaf vascular regeneration defects in *plt3;plt5-2;plt7* suggesting that it is a functional homolog of *Arabidopsis PLT* (Fig. 3H-J).

***PLT3,5,7* directly activate *CUC2* expression for wound repair and vascular regeneration**

Having established that *PLT3,5,7* regulate wound repair and vascular regeneration in damaged aerial parts of the plant, we sought to define the molecular mechanisms underlying this regulation. Previously we had shown that *PLT3,5,7* direct tissue-culture-mediated *in vitro* shoot regeneration by activating root stem cell regulators and *CUC2* (Kareem et al., 2015). While we

found no evidence for the participation of PLT1, PLT2 and WOX5 root stem cell regulators in the response to injuries in growing aerial organs (Figs S4,S9A), *CUC2* remains an attractive candidate for participation in wound repair. Therefore, we asked whether *CUC2* responds to mechanical injury and whether *PLT3,5,7* act through *CUC2* to repair wounds and regenerate vasculature.

pCUC2::3XVENUS as well as *CUC2::CUC2-vYFP* expression was detected in vascular tissue of young leaves in both wildtype and *plt3;plt5-2;plt7* mutant albeit somewhat reduced in the latter (Fig. 4A,A', Fig. S9B-F,I,I'). The same *CUC2* promoter was used to drive transcriptional and translational fusions. The detection of an expanded domain of expression of *pCUC2::3XVENUS* as compared to *CUC2::CUC2-vYFP* can be largely attributed to *3XVENUS.* Both reporter fusions used in this study can recapitulate the previously reported *CUC2* expression at the leaf margin (Nikovics et al., 2006; Bilsborough et al., 2011) (Fig. S9G,H). In response to midvein damage in wildtype, both *pCUC2::3XVENUS* as well as *CUC2::CUC2-vYFP* expression was upregulated proximal to the wound 12 h post injury followed by a broader domain of enhanced expression after 24 h in wildtype (Fig. 4B,C, Fig. S9I-K). In contrast, there was no upregulation of the reporter near the wound site in *plt3;plt5-2;plt7* (Fig. 4B',C', Fig. S9I'-K'). Similar patterns of changes were also observed at the transcript level in response to midvein injury (12 h post injury) (Fig. S9L). Similarly, in damaged inflorescence stems, *CUC2* transcripts were reduced in the *plt3;plt5-2;plt7* as compared to wildtype (Fig. 4D). Further, *CUC2* transcripts rapidly increased in injured leaves upon inducible over expression of PLT5 (*35S::PLT5-GR*) as well as of PLT7 (*35S::PLT7-GR*) even in the presence of translation inhibitor cycloheximide suggesting direct activation of *CUC2* transcription by PLT5 and PLT7 (Fig. 4E, Fig. S9M). Consistent with these observations, PLT5 binds to the *CUC2* promoter in a ChIP assay (Fig. S9N). In addition, DAP-Seq analysis identified the binding of PLT7 to *CUC2* promoter (O'Malley et al., 2016) (Fig. S10A). Furthermore, transient transfection of trans genes capable of producing PLT5 or PLT7 proteins and *CUC2* promoter driven Luciferase reporter in *Nicotiana* leaf can induce reporter expression, further demonstrating that PLT5 as well as PLT7 can directly activate *CUC2* transcription (Fig. 4F).

Since molecular data indicate that *CUC2* acts downstream of *PLT*, we asked if PLT requires *CUC2* activity for wound repair. Strikingly, inducible ectopic over expression of PLT5 failed to promote wound repair at the damaged end of *cuc2-3* mutant tissues (*cuc2-3;35S::PLT5-GR*).

The severely compromised wound repair which was observed at the cut ends remained unaltered upon PLT5 over expression in *cuc2-3* detached tissue, but not upon PLT5 over expression in wildtype (Wildtype;*35S::PLT5-GR)* which enhanced wound repair at the cut ends (Fig. S10B-F). These results demonstrate that PLT acts through *CUC2* to repair the wound.

We examined the role of *CUC2* in leaf vascular regeneration by analysing loss of function mutants. Strikingly, vascular regeneration was severely impaired in both the recessive loss-of-function *cuc2-3* mutant as well as in the *cuc2-1D* dominant mutant. 71% of *cuc2-3* mutant and 81% of *cuc2-1D* mutant leaves failed to show any vascular regeneration in response to midvein injury (Fig. 4G). Notably, loss of *CUC2* function did not cause any defect in the formation of closed vein loops formed by primary (midvein) and secondary veins (lateral veins). (Fig. S7F,G,J,K). Similarly, upon inflorescence incision, ~78% *cuc2-3* mutant and 92% of *cuc2-1D* mutant inflorescences failed to show any vascular regeneration (Fig. 4H). Finally, we asked if *CUC2* overexpression can rescue the vascular regeneration defect in *plt3;plt5-2;plt7* mutant leaves. Strikingly, the regeneration efficiency (timings of regeneration and reunion of vascular strands) as well as frequency (number of plants) was restored upon *CUC2* overexpression in *plt3;plt5-2;plt7* to the level of wildtype. New vascular strands regenerated and reunited 4 dpi in the mutant similar to wildtype (Fig. 4I-J''). Moreover, *CUC2* overexpression rescued the repair process in locally wounded *plt3;plt5-2;plt7* inflorescence stem (Fig. 4K-K''). Taken together these data demonstrate that *PLT3,5,7* directly activate *CUC2* transcription in response to injury and the *PLT-CUC2* module is required for wound repair and vascular regeneration in leaf and stem. Interestingly, *cuc2-3* mutant displayed growth of inflorescence stem similar to wildtype (Fig. S5H,K).

PLT is required for polarised cell growth and auxin response during vascular regeneration

CUC2 is implicated in the regulation of leaf margin development by directing PIN1 polarity and the resultant auxin distribution (Bilsborough et al., 2011) and PIN1 polarisation is crucial for the normal development of leaf vasculature (Scarpella et al., 2006). Hence, we next probed if the process of cell polarisation is regulated by the *PLT* transcription module during leaf vascular regeneration. We focused on *in vivo* vascular regeneration in developing leaves which has not been explored. To this end, we examined the localisation of PIN1 in response to midvein injury in the leaf blade (Fig. S11C'-F',G'-J'). Prior to wounding, we observed *PIN1::PIN1-GFP* expression in the procambium predominantly towards the basal end of

young leaves in both wildtype and mutant (Fig. S11A-F,G-J). In response to injury, we observed increased *PIN1-GFP* near wound sites in both wildtype and mutant (Fig. 11E', Fig. S11I'). To examine *PIN1-GFP* localisation in regenerating vascular cells, we generated transgenic lines harbouring both *PIN1::PIN1-GFP* and *ATHB8::ATHB8-vYFP*. ATHB8 specifically marks developing procambium cells in leaf (Scarpella et al., 2004). We observed both *PIN1-GFP* and *ATHB8-YFP* in developing procambium of 4 days old leaves (Fig. 5A,B).

During the first 12 h following incision, we did not observe regenerating vascular cells expressing both *PIN1-GFP* and *ATHB8-YFP* near wound sites (Fig. 5C,D). Regenerating procambium cells marked with *ATHB8-YFP* and polarised *PIN1-GFP* were observed after 24 h near wounds in wildtype (Fig. 5E). In contrast, we did not observe regenerating procambium cells expressing polarised *PIN1-GFP* or *ATHB8-YFP* near wound after 24 h in *plt3;plt5-2;plt7* plants demonstrating that cells surrounding the damaged site failed to re-specify the PIN1 polarity in the mutant (Fig. 5F). These data suggest that failure of re-establishment of polar auxin transport within 24 h may contribute to impaired vascular regeneration in *plt* triple mutant. We next examined if lack of directional auxin flow in the damaged *plt3;plt5-2;plt7* mutant leaves altered distribution patterns of auxin response. We examined the auxin response using the auxin reporter *pDR5::3XVENUS-N7* in both wildtype and *plt3;plt5-2;plt7* mutant plants. Prior to injury, we did not observe any difference in distribution patterns or levels of the auxin response in leaves between these two genotypes (Fig. 5G,G', Fig. S11K-M'). Both in wildtype and *plt3;plt5-2;plt7* an increase in *pDR5::3XVENUS-N7* signal in the tissue proximal to the wound was observed at 24 h post injury (Fig. 5H,H',I,I'). However a further enhanced auxin response was confined near the wound site by 48 h only in wildtype (Fig. 5J). In contrast to wildtype, the triple mutant failed to show such confined expression of *pDR5::3XVENUS-N7* signal in response to injury (Fig. 5J'). The distribution patterns and levels of auxin response in uninjured developing mutant leaves as compared to wildtype did not change, further substantiating the specific role of *PLT3,5,7* in response to injury (Fig. 5G,G', Fig. S11K-M'). Taken together, our results show that PLT3,5,7 are needed for re-specification of polarized vascular cells to facilitate vascular tissue regeneration.

PLT and CUC2 activate the transcription of local auxin biosynthesis gene in a feed forward loop to repair wound and drive vascular regeneration

Local auxin biosynthesis has been implicated in root haustoria formation and associated vascular development during host-parasite interaction (Kokla and Melnyk, 2018). We therefore

asked whether PLT2-CUC2 module regulate wound repair and vascular regeneration by modulating local auxin biosynthesis genes. Interestingly, local auxin biosynthesis genes are downregulated in *plt3;plt5-2;plt7* mutant callus (A. Kareem and K. Prasad, Unpublished data). PLT is also known to control phyllotaxis by regulating one of the auxin biosynthesis gene *YUCCA4* (*YUC4)* (Pinon et al., 2013). Similarly, *YUC4* expression was upregulated in response to midvein injury (12 h post injury) in growing wildtype leaves unlike in the *plt3;plt5-2;plt7* leaves where the transcript level reduced (Fig. 6A). In addition to damaged leaves, *YUC4* transcripts were also reduced in damaged *plt3;plt5-2;plt7* inflorescence segment (Fig. S12A). Conversely, *YUC4* transcripts were rapidly increased in injured tissues upon PLT5-GR induction (4 h) even in the presence of the translation inhibitor cycloheximide suggesting direct activation by PLT5 (Fig. 6B). Since molecular data suggests that *YUC4* acts downstream of *PLT*, we asked if PLT requires *YUC4* activity to trigger cellular reprogramming. Strikingly, inducible over expression of PLT5 as well as PLT7 failed to trigger any ectopic cellular reprogramming in *yuc4;yuc1* mutant background (*yuc4;yuc1;35S::PLT5-GR* or *yuc4;yuc1;35S::PLT7-GR)* unlike in the wildtype background (Wildtype;*35S::PLT5-GR*; *or* Wildtype;*35S::PLT7-GR*) (Fig. S12B,C). Similarly, PLT5 as well as PLT7 overexpression failed to promote wound repair at damaged ends, demonstrating that PLT acts through *YUC4* during reprogramming and wound repair (Fig. S12D-G).

We asked if in addition to *PLT*, *CUC2* can also contribute towards regulating the local auxin biosynthesis in response to injury. *YUC4* transcripts were not upregulated in response to midvein injury in the *cuc2-1D* single mutant (Fig. 6A) and its transcript levels were rapidly increased upon *CUC2-GR* induction even in the presence of the translation inhibitor cycloheximide suggesting direct activation of *YUC4* expression by CUC2 (Fig. 6C). Consistent with the likelihood of direct activation of *YUC4* transcription by CUC2 inferred from our results, DAP-Seq analysis indicated the binding of CUC2 to *YUC4* promoter (Fig. S12H) (O'Malley et al., 2016). Next we examined if, like PLT, CUC2 also requires downstream *YUC4* activity to promote vascular regeneration. Ectopic overexpression of CUC2 promoted vascular regeneration in leaf and resulted in regeneration of multiple vascular strands from the wound site in the wildtype (Wildtype;*35S::CUC2-3AT*) (Fig. 6D). In contrast to wildtype, ectopic overexpression of CUC2 failed to promote regeneration of multiple vascular strands from the wound site in *yuc4;yuc1* mutant *(yuc4;yuc1;35S::CUC2-3AT)* (Fig. 6D-F). Injured leaves in *yuc4;yuc1;35S::CUC2-3AT* seedlings either did not regenerate any vascular strand or occasionally displayed single file of regenerating vascular cells as it was observed in *yuc4;yuc1*

(Fig. 6E,F, Fig. S12I). These data demonstrate that like *PLT*, *CUC2* also acts through *YUC4* to promote wound repair and vascular regeneration.

Our data suggest that in addition to PLT, CUC2 can also activate *YUC4* expression during vascular regeneration. Activation of *YUC4* by PLT5, PLT7 as well as by CUC2 indicate a feed forward loop controlling local auxin biosynthesis (Fig. 6B,C, Fig. S12J). *PLT5-GR* can only moderately activate *YUC4* expression after 4 h induction when the function of *CUC2* and of the redundantly acting *CUC1* is lost (in damaged *cuc1-5;cuc2-3* tissues) (Fig. 6H) indicating that increased transcription of *YUC4* in wildtype damaged leaves may be an output of a coherent feed forward loop during tissue regeneration. We further provide genetic evidence for the feed forward loop wherein inducible overexpression of PLT7 or PLT5 can still increase the vascular regeneration by 18% and 24% respectively in response to midrib injury in *cuc2-3* mutant (Fig. S12K).

We further investigated this regulatory interaction by analysing the genetic interaction between *PLT* and *CUC2*. Strikingly, we found synergistic interaction between *PLT* and *CUC2* during wound repair and vascular regeneration. Cumulative loss of PLT and CUC2 function in *plt3;plt5-2;plt7;cuc2-3* mutant resulted in severely compromised wound repair at the cut end of detached plant organ as compared to *plt3;plt5-2;plt7* or *cuc2-3* mutant (Fig. S13A). In addition to dramatically reduced frequency of wound repair in *plt3;plt5-2;plt7;cuc2-3* mutant we could barely observe any proliferating callus like cells at the damaged ends in *plt3;plt5-2;plt7;cuc2-3* mutant organ (Fig. S13B-E). *YUC4* transcript level was further reduced in *plt3;plt5-2;plt7;cuc2-3* mutant as compared to *plt3;plt5-2;plt7* or *cuc2-3* mutant (Fig. S13F). Similarly, seedlings heterozygous for *plt* and *cuc2* alleles, *plt3+/-;plt5-2+/-;plt7+/-;cuc2-3+/-* displayed hypersensitivity to leaf midvein injury as compared to *plt3+/-;plt5-2+/-;plt7+/-* or *cuc2-3+/-* (Table S1). These data substantiate the regulation of YUC4 expression by PLT and CUC2 in a coherent feed forward loop during wound repair and vascular regeneration.

Consistent with the importance of activation of *YUC4* expression for regeneration, ~40% of *yuc4* single mutant and 87% of *yuc4;yuc1* double mutant leaves failed to regenerate vascular tissue in response to midvein injury (Fig. 6G). Strikingly, uninjured *yuc4* single mutant develops fully grown midvein without any discontinuity and there is no significant difference in the formation of closed vein loops as compared to wildtype (Fig. S7F,G,M). While midvein formation in *yuc4;yuc1* mutant remains normal like wildtype, the number of loops surrounding

the midvein are reduced (Fig. S7F,G,N). Strikingly, reconstitution of *YUC4* expression in the endogenous *PLT5* domain (*PLT5::YUC4-vYFP*) in *plt3;plt5-2;plt7* as well as in *cuc2-1D* mutant rescued the vascular regeneration in injured leaves to a large extent (Fig. 6I-M, Fig. S13 G-I). These data provide compelling evidence for the functional significance of *PLT-CUC2* module dependent activation of local auxin biosynthesis in controlling vascular regeneration. Remarkably, reconstitution of *YUC4* expression in *cuc1-5;cuc2-3* mutant (*cuc1-5;cuc2-3;PLT5::YUC4-vYFP*), which generates cup-shaped cotyledons but no leaf or stem, rescued post-embryonic development with fully developed rosette leaves (Fig. S14).

DISCUSSION

Multicellular organisms display the ability to regrow damaged tissues and organs. Unlike many animals where regeneration potential is restricted to specific cell lineages, plants repair and rebuild damaged tissues throughout the body. In this study, we have investigated the mechanism of wound repair across aerial parts of the plant body and we implicated PLT/AIL transcription factors, well known for their role in stem cell maintenance, as regulatory triggers for this process. We demonstrate that activation of *CUC2* transcription by PLT3,5,7 is a key regulatory mechanism of wound repair and vascular regeneration. (i) PLT binds to the *CUC2* promoter and directly activates the transcription of *CUC2*. (ii) PLT requires downstream CUC2 activity during wound repair. (iii) Reconstitution of CUC2 expression under a heterologous promoter in *plt3;plt5-2;plt7* triple mutants rescues vascular regeneration. We provide evidence that PLT and CUC2 activate the transcription of local auxin biosynthesis gene in a feed forward loop to drive vascular regeneration. (i) Both PLT and CUC2 require downstream YUC4 activity as ectopic over expression of PLT as well as of CUC2 fails to trigger regeneration response in *yuc4;yuc1* mutant. (ii) Reconstitution of YUC4 expression under heterologous promoter in *plt* triple mutant as well as in *cuc2-1D* mutant rescue the vascular regeneration defects. (iii) PLT and CUC2 act synergistically to activate *YUC4* transcription and repair the damaged tissues, which involves induction of vascular identity and proper polarization of the polar auxin transporter PIN1.

Our study revealed a previously unrecognised role of *ANT* in vascular regeneration and a *PLT*-like gene from rice, a morphologically diverse grass species, could substitute the regeneration function of *Arabidopsis PLT* genes. These observations indicate that the activation of *PLT* gene promoters in response to mechanical injuries may be more critical for the selection of regeneration-associated PLT genes than their protein sequence. In this context it is relevant that

distinct PLT transcription factors determine competence for regeneration in the root context (Durgaprasad et al., 2019).

In striking contrast to *in vitro* shoot regeneration cues (Kareem et al., 2015), *PLT3,5,7* do not act through root stem cell regulators PLT1, PLT2 and WOX5 to initiate repair of damaged aerial tissues of a growing plant. Rather, PLT acts through *CUC2* by directly activating its expression (Fig. 6N). Interestingly, *PLT* and *CUC2* acts in a feed forward loop to activate the expression of auxin biosynthesis gene *YUC4* (Fig. 6O). This circuit can act as a coherent feed forward loop which often serves as a signal persistence detector (Mangan, Zaslaver and Alon, 2003), even though our analysis indicates that the regulatory logic at the promoter is not strictly an 'AND gate' (Alon, 2006). Regardless of the precise regulatory logic, the output of the circuit is the activation of YUC4. In that view, it is tantalizing that the cellular defects associated with the malfunctioning of this circuit are the inability to redirect ground tissue cells to vascular identity and the inability to properly polarize PIN proteins. A regulatory feedback loop between auxin level, auxin flux and polarisation of auxin efflux carriers (PIN) has been proposed as a key regulatory mechanism of shoot branching, phyllotaxis and vascular tissue differentiation (Jonsson et al., 2006; Smith et al., 2006; Bayer et al., 2009; Schuetz et al., 2012; Mazur et al., 2016; Fujita and Kawaguchi, 2018). It is therefore conceivable that *PLT-CUC2*-dependent activation of YUC4 activates this feedback loop to drive vascular regeneration in damaged growing leaves (Fig. 6O). In summary our study reveals *PLT-CUC2* regulatory axis is specifically involved in controlling regeneration through induction of a local hormonal environment in response to injury.

MATERIALS AND METHODS

Detailed experimental procedures are described in supplementary information.

Plant Materials

Arabidopsis thaliana ecotype Columbia (Col-0) was used as wildtype in this study. The origins of the mutants used in the study such as double mutants *plt3;plt5-2*, *plt3;plt7*, *plt5-2;plt7* and *plt3-1*;*plt5-2*;*plt7-1* triple mutant (Prasad et al., 2011), *yuc4;yuc1* double mutant (Pinon et al., 2013), *plt3;plt7;ant4* triple mutant (Krizek, 2015), *cuc2-1D* (Larue et al., 2009) and *cuc2-3* single mutants (Hibara et al., 2006), and *cuc1-5;cuc2-3* double mutant (Hibara et al., 2006) have been described previously. Translational fusion constructs of *PLT1::PLT1-vYFP*, *PLT2::PLT2-vYFP* (Mahonen et al., 2014), *PLT3::PLT3-vYFP*, *PLT5::PLT5-vYFP* and *PLT7::PLT7-vYFP* (Prasad et al., 2011), have been described previously. *35S::PLT5-*

GR,35S::PLT7-GR (Prasad et al., 2011), *pCUC2::3XVENUS* and *35S::CUC2-3AT* (Kareem et al., 2015) have been described previously. Multisite gateway recombination cloning system (Invitrogen) using pCAMBIA 1300 destination vector was used for cloning the translational fusion constructs which were then introduced into C58 Agrobacterium strain by electroporation and further transformed into wildtype or mutants *Arabidopsis* plants by floral dip method (Clough and Bent, 1998) (See Supplementary Material and Methods for details on Plasmid construction). *DR5::VENUS* expression was examined in wildtype and *plt3;plt5-2;plt7* transgenic plants having the double markers *DR5::3XVENUS-N7, pPIN1::PIN1-GFP* line, which has been described previously (Pinon et al., 2013). In this study only the YFP marker was analysed using single YFP channel.

Growth Conditions

Arabidopsis thaliana seeds were surface sterilized with 70% ethanol and 20% bleach, followed by seven washes with sterile distilled water. Seeds were plated on half-strength Murashige-Skoog (MS) medium (pH 5.7) and grown vertically under 45 μmol/m^2s continuous white light at 22°C and 70% relative humidity.

Regeneration Assays

For wound induced natural regeneration experiments, all plants and explants were grown on hormone-free half strength MS agar medium (Sigma). To study wound repair and vascular regeneration in growing inflorescence, three weeks old seedlings were selected. Using a sterile razor blade the stem region between the rosette leaves and the first or second cauline leaves was subjected to either peeling of the tissue layers including epidermis and sub epidermal layers (inflorescence abrasion) or partial incision (inflorescence incision) through the vascular tissues under the observation of a dissection microscope (Zeiss Stemi 2000). The observations were recorded 4 days after wounding. For leaf vascular regeneration assay, to maintain uniformity, we injured a single leaf belonging to the first pair of rosette leaf of 5 dpg seedlings. Always plants of same developmental stage were chosen for incision. Fine-pointed sterile tweezers (Dumont tweezer, Style 5) were used to make a sharp incision in the midvein at the basal part of leaf blade. To avoid ambiguity, incisions made elsewhere were not scored. The incisions were made from the abaxial surface of the leaf to ensure precise injury to the midvein. The injured leaf was left connected to the growing parent plant and it was protected from any further damage. Vascular regeneration was analysed in the injured leaf 4 days post incision. These leaves were cut at the petiole using Vannas straight scissors (Ted Pella, Product

No.1340) without causing additional damage to the leaf blade. The leaf tissue was cleared using chloral hydrate (Sigma) (see supplementary Materials and Methods for further details of decolourisation and tissue clearing) and brightfield images were obtained to assess the regeneration outcomes. When newly formed vascular strands (identified by the distinct morphology of end-to-end connected xylem elements) connected the cut ends of the midvein to form a D-shaped loop or connected the damaged midvein to a lateral vein, the outcomes were scores as successful regeneration outcomes (Fig. 2I, 2J). To study healing in response to wounding in excised organs (leaf/root), excised explants were collected from 9 dpg seedlings and placed on hormone-free MS agar medium. Upon excision, continuous dexamethasone (Sigma) induction was provided till 10th day post excision for samples collected from transgenic lines harbouring steroid inducible constructs**.** The plates were kept in the dark for the first 24 to 32 h and later shifted to continuous light. All the plates of regeneration experiments were incubated vertically in a plant growth chamber maintained at 22°C and 70% relative humidity under 45 μmol/m^2s continuous white light.

Microscopic Imaging

Bright-field and confocal laser-scanning microscopy imaging were performed as described previously (Kareem et al., 2015). Brightfield images of vascular regeneration in incised leaves were acquired using bright-field mode in Leica TCS SP5 II inverted confocal microscope and Olympus BX63F after clearing the leaf sample (see supplementary Materials and Methods for details of decolourisation and tissue clearing). Confocal imaging of leaves and thick samples were performed using Leica TCS SP5 II upright microscope and Zeiss LSM 880 confocal laser scanning microscope. Brightfield images acquired using Leica M205 FA fluorescence stereo microscope and confocal microscopes were adjusted for brightness and contrast. For confocal imaging, the cell boundaries of root, hypocotyls and callus samples were stained using 10 μg/ml propidium iodide (Sigma). Images were acquired using 10x air objective, 20x oil immersion, 20x air objective and 40x oil immersion objectives. The projection view of the images was reconstructed from the Z stacks with Leica LAS-AF software and Zeiss ZEN blue softwares. Images were compiled using Adobe Photoshop CS6. All image panels represent Z stack unless mentioned. Area of callus formation at the cut end of detached organs were measured using ImageJ software.

qRT-PCR

Total RNA was extracted from samples (see supplementary Materials and Methods for further details of sample preparation) using Nucleospin Plant RNA extraction kit (MN) and subjected to on-column DNase treatment according to the manufacturer's guidelines. cDNA was synthesized from 1 µg total RNA using a High-Capacity cDNA Reverse Transcription kit (Applied Biosystems). qRT-PCR was performed in 25 µl reaction volume containing 12.5 µl SYBR Green PCR master mix (Takara), 100 nM gene-specific primers (Table S1) and 100 ng cDNA in CFX96 Touch™ Real-Time PCR Detection System. All reactions were performed with RNA derived from three independent biological replicates. Each biological sample was tested in technical triplicate. *ACTIN2* (*ACT2*) was used to normalize the result. Transcript level in control was always normalised to 1. The expression of the gene of interest is represented with respect to the control (as performed in Kareem et al., 2015). The relative gene expression was represented as fold-change value by calculating $-\Delta\Delta C^{T}$.

Luciferase Assay

Luciferase assay was performed as decribed in (Díaz-Triviño et al., 2017). 3-4 weeks old healthy *Nicotiana benthamiana* plants grown under long day condition (16 h light, 8 h dark) were used for agroinfiltration. The primer used for cloning are listed in Table S2. Competent cells of EHA105 and ABI strains of *Agrobacterium tumefaciens* were used for the infiltration.

ChIP-qPCR Analysis.

ChIP was performed by following the protocol as described in (Yamaguchi et al., 2014) (see supplementary Materials and Methods for a brief description and primer details). ChIP-qPCR was performed using SYBR Premix (Clontech) to determine the PLT5 protein occupancy on *CUC2* promoter region. The relative fold enrichment of CUC2 DNA was calculated by computing the enrichment in *PLT5::PLT5-vYFP* relative to *plt3;plt5;plt7*. ACTIN7 (ACT7) was used to normalise the results between the samples. The ChIP-qPCR reactions were performed in triplicates. The primers used for ChIP-qPCR are listed in supplementary table S3.

Statistical Analysis

Pearson's chi-squared test (regeneration assay analysis), Welch two sample *t*-test (qRT-PCR data analysis), Mann-Whitney U1-tailed test (Luciferase assay) and Kruskal-Wallis chi-squared test (comparing number of closed vein loops) were used for data analysis. Holm-

bonferroni correction was performed for multiple analysis while using Pearson's chi-squared test. R programme was used for the statistical analyses.

ACKNOWLEDGEMENTS

We thank Dr. Philip N. Benfey, Dr. Elliot Meyerowitz, and Dr. Ottoline Leyser for their valuable suggestions on the early draft of the manuscript. We are grateful to Dr. Charles Melnyk and Dr. Utpal Nath for all the discussions and help. *pG10-90:vYFP* control vector for luciferase assay was received from Menno Pijnenburg. We are thankful to Krishnaprashanth M.K. for assistance with schematics and figures, Subhiksha B. for cloning *AtPLT5::OsPLT2-vYFP* and to Sajesh Vijayan for help with the statistical analyses.

COMPETING INTERESTS

No competing interests declared.

FUNDING

KP acknowledges grants from the Department of Biotechnology (DBT), Government of India [grant# BT/PR12394/AGIII/103/891/2014] and Department of Science and Technology-Science and Engineering Research Board (DST-SERB), Government of India [grant# EMR/2017/002503/PS] and also acknowledges IISER-TVM for infrastructure and financial support. DR acknowledges University Grants Commission (UGC) fellowship. APS, VV and AT are recipients of Council of Scientific and Industrial Research (CSIR) fellowship. MA acknowledges Department of Biotechnology (DBT), Ministry of Science and Technology, Government of India for granting the DBT-Post Doctoral Fellowship (DBT-RA Program). APM acknowledges grants from the Academy of Finland [grants #266431, #271832]. IE acknowledges the Israeli Science Foundation [# ISF966/17] and the Howard Hughes Medical Institute [International Research Scholar Grant #55008730]. BAK was supported by a grant from National Science Foundation (NSF) [grant #NSFIOS135442]. ES was supported by Discovery Grants of the Natural Science and Engineering Research Council of Canada (grants #NSERC RGPIN-2016-04736 and #NSERC RGPAS 492872-2016.

DATA AVAILABILITY

All raw data associated with this manuscript have been deposited in Mendeley (https://data.mendeley.com/datasets/mwyxw4v63h/draft?a=e64505aa-564b-4127-9d0c-afc900810544). Reserved doi:10.17632/mwyxw4v63h.1

AUTHOR CONTRIBUTIONS

AK, KP conceived the research; AK, DR, APS and KP designed the research; DR, AK, APS, MA, VV, AT, DV, ANL performed all the experiments at IISER TVM, except *Nicotiana* leaf agroinfiltration and luciferase reporter induction which were performed by MK and VW; DR, AK, APS, MA, AT, AS, MKM, VW, BS and KP analyzed the data; AK, DR and APS prepared the first draft of the manuscript, wrote figure legends and methods; KP and BS revised and edited the manuscript. All the co-authors commented on the manuscript; BAK, APM, IE, MGS, and ES contributed important reagents.

REFERENCES

Alon, U. (2006). *An Introduction to Systems Biology*. New York: Chapman and Hall/CRC. https://doi.org/10.1201/9781420011432

Asahina, M., Azuma, K., Pitaksaringkarn, W., Yamazaki, T., Mitsuda, N., Ohme-Takagi, M., Yamaguchi, S., Kamiya, Y., Okada, K., Nishimura, T. et al. (2011). Spatially selective hormonal control of RAP2.6L and ANAC071 transcription factors involved in tissue reunion in Arabidopsis. *Proc. Natl. Acad. Sci. USA* **108**, 16128-16132. doi: 10.1073/pnas.1110443108.

Bayer, E.M., Smith, R.S., Mandel, T., Nakayama, N., Sauer, M., Prusinkiewicz, P. and Kuhlemeier, C. (2009). Integration of transport-based models for phyllotaxis and midvein formation. *Genes Dev*. **23**, 373-384. doi: 10.1101/gad.497009.

van den Berg, C., Willemsen, V., Hage, W., Weisbeek, P. and Scheres, B. (1995). Cell fate in the Arabidopsis root meristem determined by directional signalling. *Nature* **378**, 62-65. doi: 10.1038/378062a0.

Bilsborough, G.D., Runions, A., Barkoulas, M., Jenkins, H.W., Hasson, A., Galinha, C., Laufs, P., Hay, A., Prusinkiewicz, P. and Tsiantis, M. (2011). Model for the regulation of Arabidopsis thaliana leaf margin development. *Proc. Natl. Acad. Sci. USA* **108**, 3424-3429. doi: 10.1073/PNAS.1015162108.

Clough, S. J. and Bent, A. F. (1998). Floral dip: a simplified method for Agrobacterium-mediated transformation of Arabidopsis thaliana. *The Plant Journal* **16**, 735-743. doi: 10.1046/j.1365-313x.1998.00343.x.

Díaz-Triviño, S., Long, Y., Scheres, B. and Blilou, I. (2017). Analysis of a plant transcriptional regulatory network using transient expression systems. In *Methods in Molecular Biology*, pp. 83-103. Humana Press. doi: 10.1007/978-1-4939-7125-1_7.

Donner, T. J., Sherr, I. and Scarpella, E. (2009). Regulation of preprocambial cell state acquisition by auxin signaling in Arabidopsis leaves. *Development* **136**, 3235–3246. doi: 10.1242/dev.037028.

Du, Y. and Scheres, B. (2017). PLETHORA transcription factors orchestrate de novo organ patterning during Arabidopsis lateral root outgrowth. *Proc. Natl. Acad. Sci. USA* **114**, 11709-11714.

Durgaprasad, K., Roy, M.V., Venugopal, A., Kareem, A., Raj, K., Willemsen, V., Mähönen, A.P., Scheres, B. and Prasad, K. (2019). Gradient expression of transcription factor imposes a boundary on organ regeneration potential in plants. *Cell Rep*. **29**, 453-463. doi: 10.1016/j.celrep.2019.08.099.

Efroni, I., Mello, A., Nawy, T., Ip, P.L., Rahni, R., DelRose, N., Powers, A., Satija, R. and Birnbaum, K.D. (2016). Root regeneration triggers an embryo-like sequence guided by hormonal interactions. *Cell* **165**, 1721-1733. doi: 10.1016/j.cell.2016.04.046.

Flaishman, M. A., Loginovsky, K. and Lev-Yadun, S. (2003). Regenerative xylem in inflorescence stems of Arabidopsis thaliana. *J. Plant Growth Regul*. **22**, 253-258. doi: 10.1007/s00344-003-0030-y.

Fujita, H. and Kawaguchi, M. (2018). Spatial regularity control of phyllotaxis pattern generated by the mutual interaction between auxin and PIN1. *PLoS Comput. Biol*. **14**, 1-23. doi: 10.1371/journal.pcbi.1006065.

Galliot, B., Crescenzi, M., Jacinto, A. and Tajbakhsh, S. (2017). Trends in tissue repair and regeneration. *Development* **144**, 357-364. doi: 10.1242/dev.144279.

Hibara, K.I., Karim, M.R., Takada, S., Taoka, K.I., Furutani, M., Aida, M. and Tasaka, M. (2006). Arabidopsis CUP-SHAPED COTYLEDON3 regulates postembryonic shoot meristem and organ boundary formation. *Plant Cell* **18**, 2946-2957. doi: 10.1105/tpc.106.045716.

Hibara, K.I., Karim, M.R., Takada, S., Taoka, K.I., Furutani, M., Aida, M. and Tasaka, M. (2016). Plant regeneration: cellular origins and molecular mechanisms. *Development* **143**, 1442-1451. doi: 10.1242/dev.134668.

Ikeuchi, M., Shibata, M., Rymen, B., Iwase, A., Bågman, A.M., Watt, L., Coleman, D., Favero, D.S., Takahashi, T., Ahnert, S.E. et al. (2018). A gene regulatory network for cellular reprogramming in plant regeneration. *Plant Cell Physiol*. **59**, 765–777. doi: 10.1093/pcp/pcy013.

Jönsson, H., Heisler, M.G., Shapiro, B.E., Meyerowitz, E.M. and Mjolsness, E. (2006). An auxin-driven polarized transport model for phyllotaxis. *Proc. Natl. Acad. Sci. USA* **103**, 1633–1638. doi: 10.1073/pnas.0509839103.

Kareem, A., Durgaprasad, K., Sugimoto, K., Du, Y., Pulianmackal, A.J., Trivedi, Z.B., Abhayadev, P.V., Pinon, V., Meyerowitz, E.M., Scheres, B. et al. (2015). PLETHORA genes control regeneration by a two-step mechanism. *Curr. Biol.* **25**, 1017–1030. doi: 10.1016/j.cub.2015.02.022.

Kokla, A. and Melnyk, C. W. (2018). Developing a thief: Haustoria formation in parasitic plants. *Dev. Biol.* **442**, 53–59. doi: 10.1016/j.ydbio.2018.06.013.

Krizek, B. A. (2015). AINTEGUMENTA-LIKE genes have partly overlapping functions with AINTEGUMENTA but make distinct contributions to Arabidopsis thaliana flower development. *J. Exp. Bot.* **66**, 4537–4549. doi: 10.1093/jxb/erv224.

Larue, C. T., Wen, J. and Walker, J. C. (2009). A microRNA-transcription factor module regulates lateral organ size and patterning in Arabidopsis. *The Plant Journal* **58**, 450–463. doi: 10.1111/j.1365-313X.2009.03796.x.

Mähönen, A.P., Ten Tusscher, K., Siligato, R., Smetana, O., Díaz-Triviño, S., Salojärvi, J., Wachsman, G., Prasad, K., Heidstra, R. and Scheres, B. (2014). PLETHORA gradient formation mechanism separates auxin responses. *Nature* **515,** 125. doi: 10.1038/nature13663.

Mangan, S., Zaslaver, A. and Alon, U. (2003). The coherent feedforward loop serves as a sign-sensitive delay element in transcription networks. *J. Mol. Biol.* **334**, 197-204. doi: 10.1016/j.jmb.2003.09.049.

Marhava, P., Hoermayer, L., Yoshida, S., Marhavý, P., Benková, E. and Friml, J. (2019) Re-activation of stem cell pathways for pattern restoration in plant wound healing. *Cell*. **177**, 957-969. doi: 10.1016/j.cell.2019.04.015.

Mazur, E., Benková, E. and Friml, J. (2016). Vascular cambium regeneration and vessel formation in wounded inflorescence stems of Arabidopsis. *Sci. Rep.* **6**, 33754.

Melnyk, C.W., Schuster, C., Leyser, O. and Meyerowitz, E.M. (2015). A developmental framework for graft formation and vascular reconnection in Arabidopsis thaliana. *Curr. Biol.* **25,** 1306-18. doi: 10.1016/j.cub.2015.03.032.

Nikovics, K., Blein, T., Peaucelle, A., Ishida, T., Morin, H., Aida, M. and Laufs, P. (2006). The balance between the MIR164A and CUC2 genes controls leaf margin serration in Arabidopsis. *The Plant Cell* **18**, 2929-2945. doi: 10.1105/TPC.106.045617.

O'Malley, R.C., Huang, S.S.C., Song, L., Lewsey, M.G., Bartlett, A., Nery, J.R., Galli, M., Gallavotti, A. and Ecker, J.R. (2016). Cistrome and epicistrome features shape the regulatory DNA landscape. *Cell* **165**, 1280-1292. doi: 10.1016/j.cell.2016.04.038.

Ohashi-Ito, K., Oguchi, M., Kojima, M., Sakakibara, H. and Fukuda, H. (2013). Auxin-associated initiation of vascular cell differentiation by LONESOME HIGHWAY. *Development* **140**, 765-769. doi: 10.1242/dev.087924.

Pinon, V., Prasad, K., Grigg, S.P., Sanchez-Perez, G.F. and Scheres, B. (2013). Local auxin biosynthesis regulation by PLETHORA transcription factors controls phyllotaxis in Arabidopsis. *Proc. Natl. Acad. Sci. USA* **110,** 1107-1112. doi: 10.1073/pnas.1213497110.

Pitaksaringkarn, W., Matsuoka, K., Asahina, M., Miura, K., Sage- Ono, K., Ono, M., Yokoyama, R., Nishitani, K., Ishii, T., Iwai, H. et al. (2014). *XTH20* and *XTH19* regulated by ANAC071 under auxin flow are involved in cell proliferation in incised Arabidopsis inflorescence stems. *The Plant Journal* **80**, 604-614. doi: 10.1111/tpj.12654.

Prasad, K., Grigg, S.P., Barkoulas, M., Yadav, R.K., Sanchez-Perez, G.F., Pinon, V., Blilou, I., Hofhuis, H., Dhonukshe, P., Galinha, C. et al. (2011). Arabidopsis PLETHORA transcription factors control phyllotaxis. *Curr. Biol.* **21**, 1123-1128. doi: 10.1016/j.cub.2011.05.009.

Radhakrishnan, D., Kareem, A., Durgaprasad, K., Sreeraj, E., Sugimoto, K. and Prasad, K. (2018). Shoot regeneration: a journey from acquisition of competence to completion. *Curr. Opin. Plant Biol.* **41,** 23-31. doi: https://doi.org/10.1016/j.pbi.2017.08.001.

Reinhardt, D., Frenz, M., Mandel, T. and Kuhlemeier, C. (2003). Microsurgical and laser ablation analysis of interactions between the zones and layers of the tomato shoot apical meristem. *Development* **130**, 4073-83. doi: 10.1242/DEV.00596.

Sachs, T. (1968). On the determination of the pattern of vascular tissue in peas. *Ann. Bot*. **32,** 781-790. doi: 10.1093/oxfordjournals.aob.a084249.

Sachs, T. (1969). Polarity and the induction of organized vascular tissues. *Ann. Bot*. **33**, 263-275. doi: 10.1093/oxfordjournals.aob.a084281.

Sachs, T. (1981). The Control of the Patterned Differentiation of Vascular Tissues. In *Advances in Botanical Research*, pp. 151–262. Academic Press. doi: 10.1016/S0065-2296(08)60351-1.

Sachs, T. (1991). *Pattern Formation in Plant Tissues*. New York: Cambridge University Press.

Scarpella, E., Francis, P. and Berleth, T. (2004). Stage-specific markers define early steps of procambium development in Arabidopsis leaves and correlate termination of vein formation with mesophyll differentiation. *Development* **131**, 3445-3455.doi: 10.1242/dev.01182.

Scarpella, E., Marcos, D., Friml, J. and Berleth, T. (2006). Control of leaf vascular patterning by polar auxin transport. *Genes Dev*. **20**, 1015-1027. doi: 10.1101/gad.1402406.

Schuetz, M., Smith, R. and Ellis, B. (2012). Xylem tissue specification, patterning, and differentiation mechanisms. *J. Exp. Bot.* **64**, 11-31. doi: 10.1093/jxb/ers287.

Smetana, O., Mäkilä, R., Lyu, M., Amiryousefi, A., Rodriguez, F.S., Wu, M.F., Solé-Gil, A., Gavarron, M.L., Siligato, R., Miyashima, S. et al. (2019). High levels of auxin signalling define the stem-cell organizer of the vascular cambium. *Nature* **565**, 485–489. doi: 10.1038/s41586-018-0837-0.

Smith, R.S., Guyomarc'h, S., Mandel, T., Reinhardt, D., Kuhlemeier, C. and Prusinkiewicz, P. (2006). A plausible model of phyllotaxis. *Proc. Natl. Acad. Sci. USA* **103**, 1301–1306. doi: 10.1073/pnas.0510457103.

Wenzel, C.L., Schuetz, M., Yu, Q. and Mattsson, J. (2007). Dynamics of MONOPTEROS and PIN-FORMED1 expression during leaf vein pattern formation in Arabidopsis thaliana. *The Plant Journal* **49**, 387-98. doi: 10.1111/j.1365-313X.2006.02977.x.

Xu, J., Hofhuis, H., Heidstra, R., Sauer, M., Friml, J. and Scheres, B. (2006). A molecular framework for plant regeneration. *Science*. **311**, 385-388. doi: 10.1126/science.1121790.

Yamaguchi, N., Winter, C.M., Wu, M.F., Kwon, C.S., William, D.A. and Wagner, D. (2014). PROTOCOL: Chromatin Immunoprecipitation from Arabidopsis Tissues, In *The Arabidopsis Book*, p.12, e0170. doi: 10.1199/tab.0170.

Zhou, W., Lozano-Torres, J.L., Blilou, I., Zhang, X., Zhai, Q., Smant, G., Li, C. and Scheres, B. (2019). A jasmonate signaling network activates root stem cells and promotes regeneration. *Cell*. **177**, 942-956. doi: 10.1016/j.cell.2019.03.006

Figures

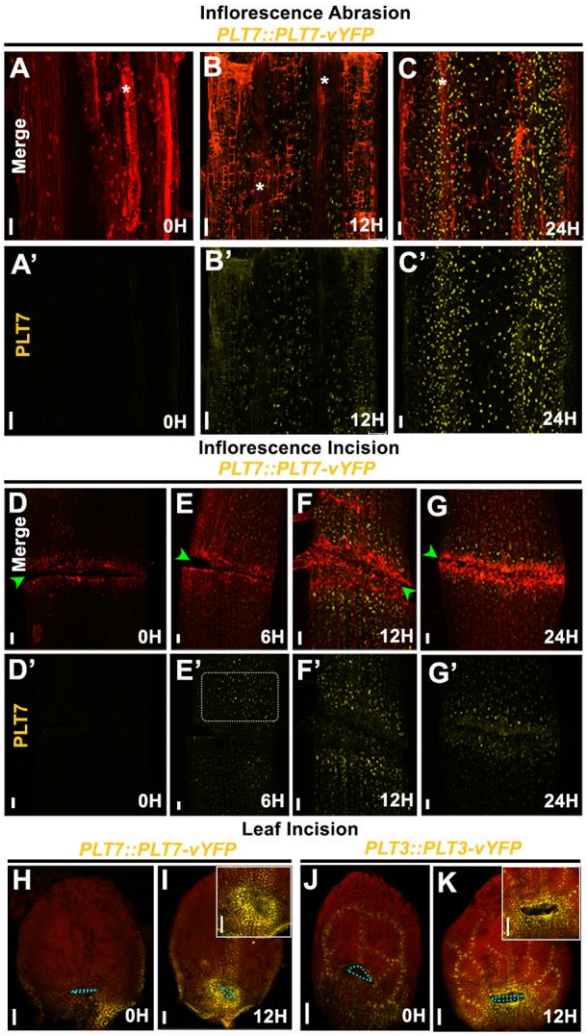

Fig. 1. *PLT3, PLT5* and PLT7 genes are locally induced after mechanical injury.

(A-G, A'-G') *PLT7::PLT7-vYFP* expression (yellow) post abrasion (A-C') and partial incision (green arrowhead) in growing inflorescence (D-G'). White asterisks: vascular tissues exposed by damage to epidermal and sub-epidermal layers following local abrasion. E' white dotted area: Upregulation of *PLT7* expression at upper end of cut. (A'-C' and D'-G'): maximum intensity projection of Z stack in YFP channel corresponding to (A-C and D-G).

(H-K) Upregulation of *PLT7::PLT7-vYFP* (H,I) and *PLT3::PLT3-vYFP* (J,K) (yellow) near wound site (insets) following leaf incision (blue dotted area: incision site). The panels represent different samples at each time point. Red signal is propidium iodide staining in (A-G) and chlorophyll autofluorescence in (H-K). Scale bars:50 μm. Brightness of YFP signal increased for visibility in panels B' and E'.

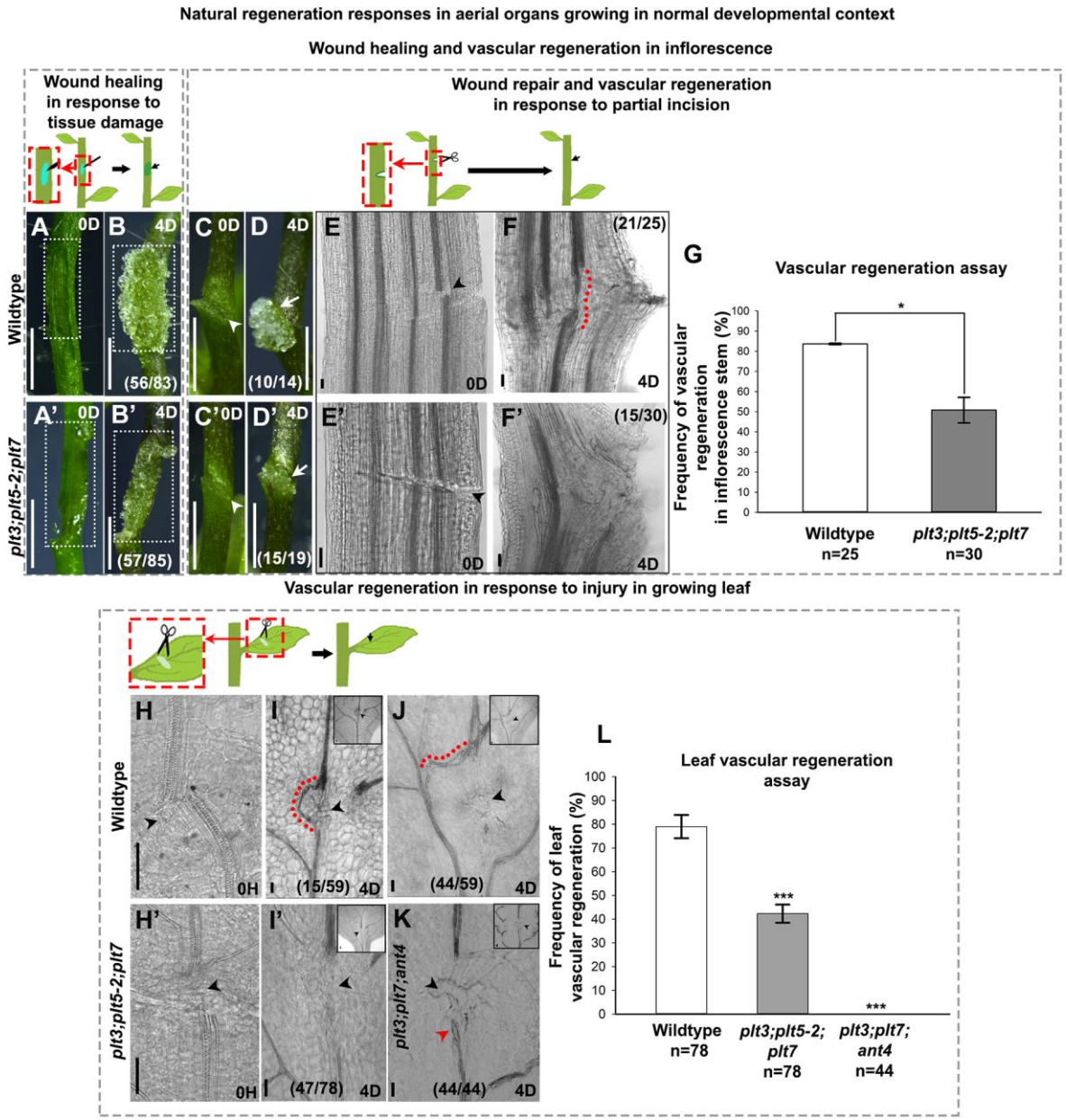

Fig. 2. *PLT* activates innate regenerative responses to injuries in aerial organs growing in the normal developmental-context.

(A-F, A'-F') Wound healing and vascular regeneration in inflorescence. (A, A') Abrasion (dotted rectangle) in inflorescence stem of wildtype (A) and *plt3;plt5-2;plt7* (A'). (B, B') Reduced wound healing response (dotted rectangle: cell proliferation) in *plt3;plt5-2;plt7* (B') as compared to wildtype (B). (C, C') Partial incision (white arrowhead) in inflorescence stem of wildtype (C) and *plt3;plt5-2;plt7* (C'). (D, D') Compromised callus formation (white arrow) in inflorescence stem of *plt3;plt5-2;plt7* (D') as compared to wildtype (D). (E, E') Disruption of vascular tissue (black arrowhead) by partial incision in inflorescence stem of wildtype (E)

and *plt3;plt5-2;plt7* (E'). (F, F') Vascular strands regenerate in wildtype inflorescence stem (F) but fail to regenerate in ~49% of *plt3;plt5-2;plt7* inflorescence stems (F').

(G) Frequency of vascular regeneration in response to partial incision in the inflorescence stem of wildtype and *plt3;plt5-2;plt7* (**p*=0.033).

(H-K, H', I') Vascular strand regeneration in growing leaf. (H, H') Incision (black arrowhead) in the midvein of wildtype (H) and *plt3;plt5-2;plt7* (H') growing leaf. (I) Vascular strand regenerate in wildtype leaf, bypassing wounded area and connecting cut ends of midvein. (J) New vascular strand connects upper cut end of midvein to lateral vein. (I', K) Vascular strand failed to regenerate in 60% of *plt3;plt5-2;plt7* (I') leaves. *plt3;plt7;ant4* (K) mutant leaves completely failed to regenerate in response to midvein injury. Red arrowhead (K): proliferating cells at lower cut end of midvein. Insets: zoomed out images of site of injury. Black arrowhead in (H-K and H', I'): incision site. (L) Frequency of leaf vascular regeneration in wildtype, *plt3;plt5-2;plt7*(***p=1.211x10^{-15}) and *plt3;plt7;ant4* mutants (***p=7.707x10^{-13}).

Red dotted line: Regenerated vascular strand. Scale bar:1 mm in A-D and A'-D'. In remaining panels scale bars represent 50 µm. Parenthesis: sample number.

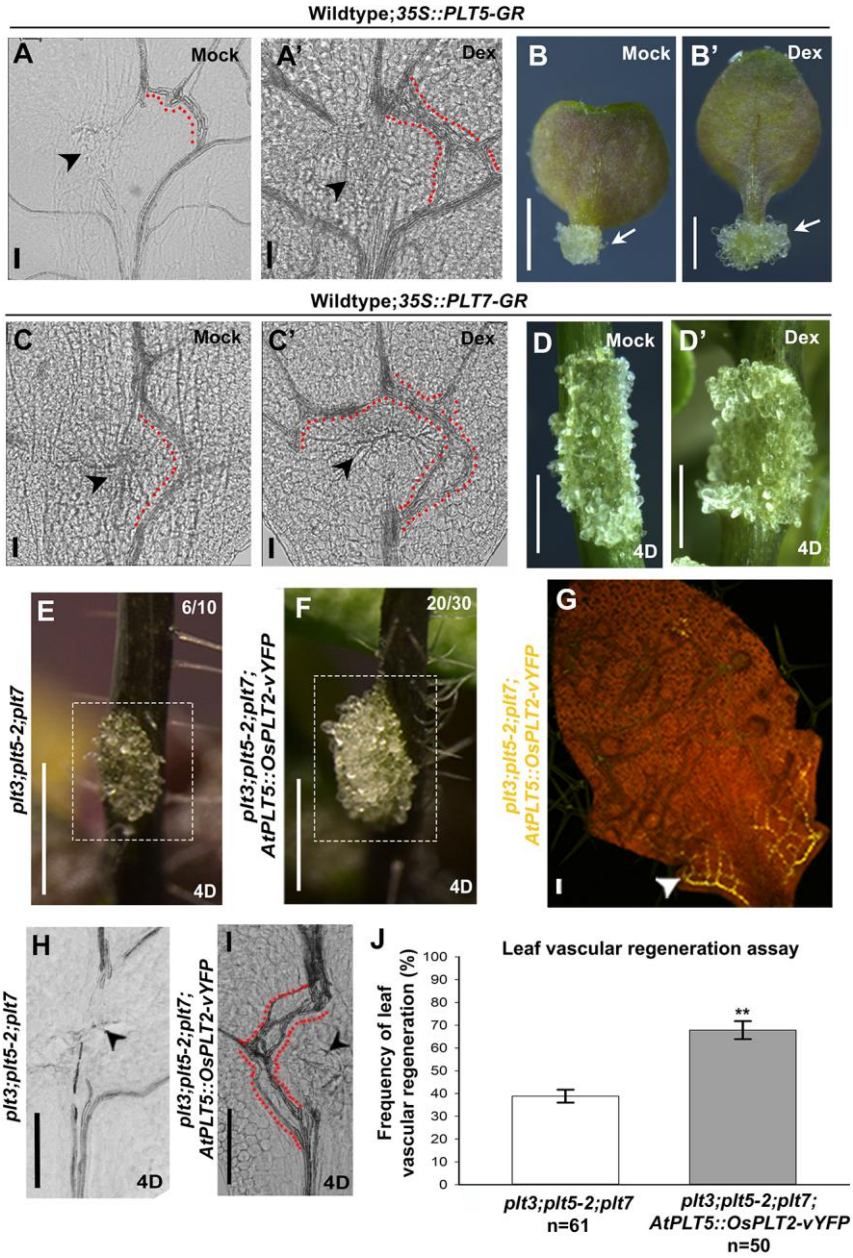

Fig. 3. *PLT* is sufficient for enhancing vascular regeneration and wound repair.

(A-B') Overexpression of *35S::PLT5-GR* promotes multiple vascular strand (A') formation upon leaf incision and callus formation (white arrows) at cut end of detached organ (B') unlike in mock treated control (A, B). (C-D') Overexpression of *35S::PLT7-GR* enhances multiple strand formation upon leaf incision (C') and wound repair upon inflorescence abrasion (D') unlike in mock treated control (C, D). (E, F) Only residual cell proliferation response is observed in *plt3;plt5-2;plt7* (E) unlike extensive callus like growth observed in *plt3;plt5-2;plt7;AtPLT5::OsPLT2-vYFP* (F) in response to inflorescence abrasion. Dotted rectangle: cell proliferation.

(G) Expression of *AtPLT5::OsPLT2-vYFP* in vascular tissue (white arrowhead) of *plt3;plt5-2;plt7 l*eaf.

(H-J) Rescue of vascular tissue regeneration in response to leaf incision in *plt3;plt5-2;plt7;AtPLT5::OsPLT2-vYFP* (I, J) (**p=0.004) while ~61% *plt3;plt5-2;plt7* (H) leaves failed to regenerate.

Black arrowhead: Incision site. Red dotted lines: Regenerated vascular strand. Scale bar: 50 μm in all images except in B, B' and D-F: scale bars represent 1mm.

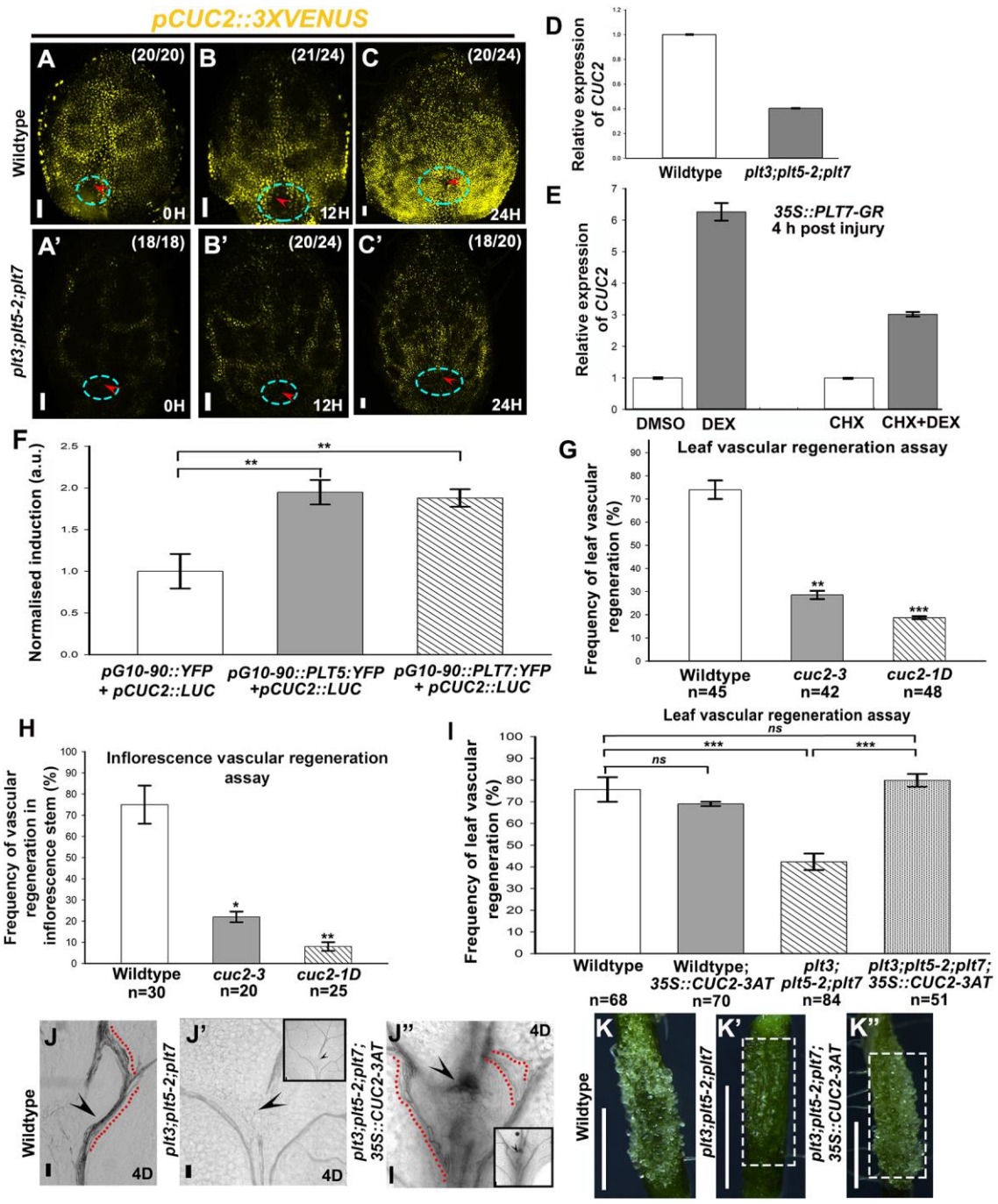

Fig. 4. *PLT* acts through *CUC2* to repair wound and to regenerate vascular tissue.

(A-C, A'-C') Reduced expression of *pCUC2::3XVENUS* (yellow) in *plt3;plt5-2;plt7* (A'-C') as compared to wildtype (A-C) in response to injury. Red arrowheads denote incision site and dashed circles enclose leaf tissue in the vicinity of the wound showing upregulation of *pCUC2::3XVENUS* in wildtype unlike in *plt3;plt5-2;plt7*. (D) Relative expression levels (qRT-PCR) of *CUC2* in injured *plt3;plt5-2;plt7* mutant inflorescence segment compared to wildtype (4 days post injury). (E) Rapid upregulation of *CUC2* (qRT-PCR) in injured tissue upon

induction of *35S::PLT7-GR*. Expression levels in D and E are normalized to ACTIN2. Error bar represents s.e.m. from three independent biological replicates. (F) PLT5 and PLT7 induce *pCUC2* in a LUC reporter assay 2 days post inoculation in *Nicotiana*. Asterisks (**) indicate $0.01 > p > 0.001$ in a Mann-Whitney U 1-tailed test. (G) Frequency of leaf vascular regeneration in *cuc2-3* (recessive) (**p=0.007), *cuc2-1D* (dominant) (***p=0.0005) mutants as compared to wildtype. (H) Frequency of vascular regeneration in response to partial incision in the inflorescence stem of wildtype, *cuc2-3* and *cuc2-1D* (*p=0.02, **p=0.001) (I) Frequency of leaf vascular regeneration in wildtype, wildtype;*35S::CUC2-3AT* (ns;p=0.65), *plt3;plt5-2;plt7* (***$p=9.9x10^{-5}$) and *plt3;plt5-2;plt7;35S::CUC2-3AT* (***$p=4.7x10^{-6}$). (J-J'') Wildtype represented as (J). Vascular tissue regeneration is rescued in *plt3;plt5-2;plt7;35S::CUC2-3AT* (J'') as compared to *plt3;plt5-2;plt7* (J') in response to leaf incision (black arrowhead). Note the increased vascular strand proliferation and regeneration of multiple vascular strands (red dotted lines) generating multiple reunion points in *plt3;plt5-2;plt7;35S::CUC2-3AT* (J'') unlike in *plt3;plt5-2;plt7* (J'). (J' and J'' (insets): incision site). (K-K'') Wildtype is represented as (K). Ectopic overexpression of *CUC2* in *plt3;plt5-2;plt7 (plt3;plt5-2;plt7;35S::CUC2-3AT)* (K'') enhances local cell proliferation and wound healing response upon inflorescence abrasion (enclosed in dotted rectangle) as compared to *plt3;plt5-2;plt7* (K'). The scale bars in (K-K'') represent 1mm while in the rest it represents 50 μm.

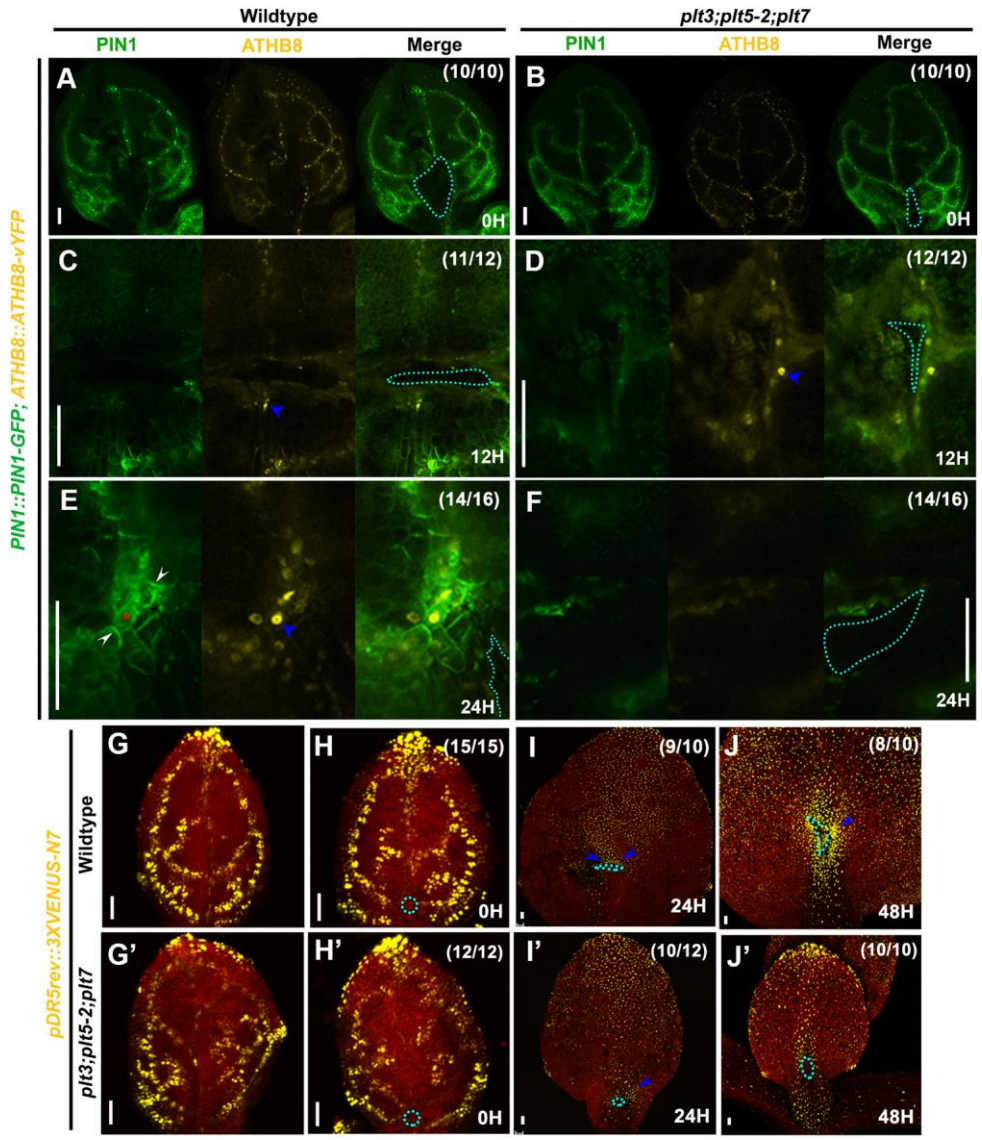

Fig. 5. *PLT* regulates polarised cell growth and auxin response during vascular regeneration.

(A-F) Expression of *PIN1::PIN1-GFP* and *ATHB8::ATHB8-vYFP* in wildtype (A, C, E) and *plt3;plt5-2;plt7* (B, D, F) mutant leaves in response to leaf incision. (A, B) YFP channel: Expression of *ATHB8::ATHB8-vYFP* in procambium cells of leaf. (C, D) No expression of PIN1 is detected in the immediate vicinity of the wound at 12 h in both wildtype (C) and *plt3;plt5-2;plt7* (D). Pre-existing ATHB8 (blue arrowheads) expression is observed near wound (in C and D YFP channel). (E, F) Expression of polarised *PIN1::PIN1-GFP* (white arrowhead) and *ATHB8::ATHB8-vYFP* (blue arrowhead) in the regenerating cells (hexagonal developing procambium cells- red asterisk) of wildtype. PIN1 polarisation and ATHB8 expression is absent in *plt3;plt5-2;plt7* (F). Blue dotted area: Tissue damaged by leaf incision.

Brightness of YFP channel (representing ATHB8) signal increased for visibility in (A-F). (A-F) represent subset of Z stack sections.

(G, G') *pDR5::3XVENUS-N7* expression in undamaged leaves of wildtype (G) and *plt3;plt5-2;plt7* (G'). (H-J, H'-J') *pDR5::3XVENUS-N7* expression in wildtype (H-J) and *plt3;plt5-2;plt7* (H'-J') leaves post incision (dotted area: incision site). Note the confined expression of *pDR5::3XVENUS-N7* in the tissue around the wound (blue arrowheads) in wildtype (J) unlike in *plt3;plt5-2;plt7* (J'). Scale bars: 50 μm. Red colour in G-J' represent chlorophyll autofluorescence.

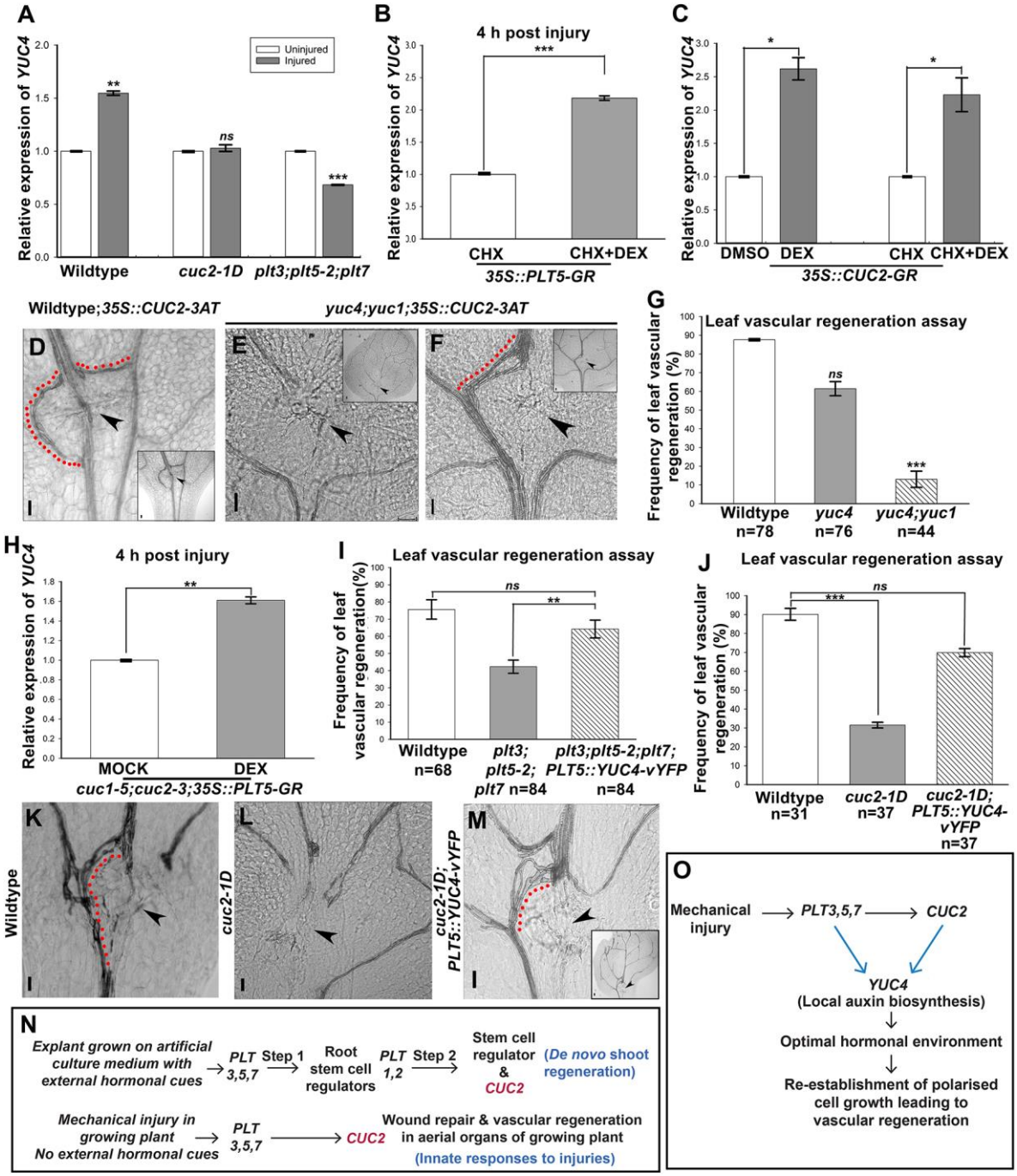

Fig. 6. *PLT* and *CUC2* dependent auxin biosynthesis drives vascular regeneration in leaf. (A) *YUC4* transcript level in wildtype, *cuc2-1D*, *plt3;plt5-2;plt7* injured and uninjured leaves, measured by qRT-PCR (**p=0.001, ns=0.45, ***p=0.0002). (B) Upregulation of *YUC4* (qRT-PCR) transcript level in injured leaves upon induction of *35S::PLT5-GR* with cycloheximide (CHX) treatment (***p=0.0008). (C) Upregulation of *YUC4* (qRT-PCR) transcript levels in injured leaves upon induction of *35S::CUC2-GR* with and without CHX treatment. (*p<0.05) (D-F) Ectopic overexpression of CUC2 produced multiple vascular strands from the wound

site in the wildtype;*35S::CUC2-3AT* (D) unlike in *yuc4;yuc1;35S::CUC2-3AT* (E, F). (G) Percentage of leaf vascular regeneration in wildtype, *yuc4* (ns;p=0.8) and *yuc4;yuc1* (***p=1.02x10^{-6}).

(H) *YUC4* transcript level in *cuc1-5;cuc2-3* upon induction of *35S::PLT5-GR*, measured by qRT-PCR. (A-C,H) are normalized to ACTIN2. Error bar represents s.e.m. from three independent biological replicates (**p=0.0032).

(I) Frequency of leaf vascular regeneration in wildtype, *plt3;plt5-2;plt7* (ns=0.18) and *plt3;plt5-2;plt7;PLT5::YUC4-vYFP* (**p=0.0087).

(J-M) Reconstitution of local auxin biosynthesis gene in *PLT5* domain rescues leaf vascular regeneration in *cuc2-1D* mutant (***p=4.11x10^{-6}, ns=0.08)

Black arrowheads: incision site. Red dotted lines: Regenerated vascular strands. Scale bar:50 µm

(N) Schematic showing *PLT-CUC2* module independently activating innate regeneration responses to injuries unlike sequential activation of CUC2 after activation of root stem cell regulators during *de novo* shoot regeneration.

(O) Schematic representing the mechanistic module of *PLT* transcription factors activating *CUC2* and *YUC4* to generate an optimal auxin environment to aid in re-establishment of polarised growth of vascular cells. Regulatory interactions marked using light blue arrows emerged from present study and was not known previously in any regeneration context.

SUPPLEMENTARY FIGURES

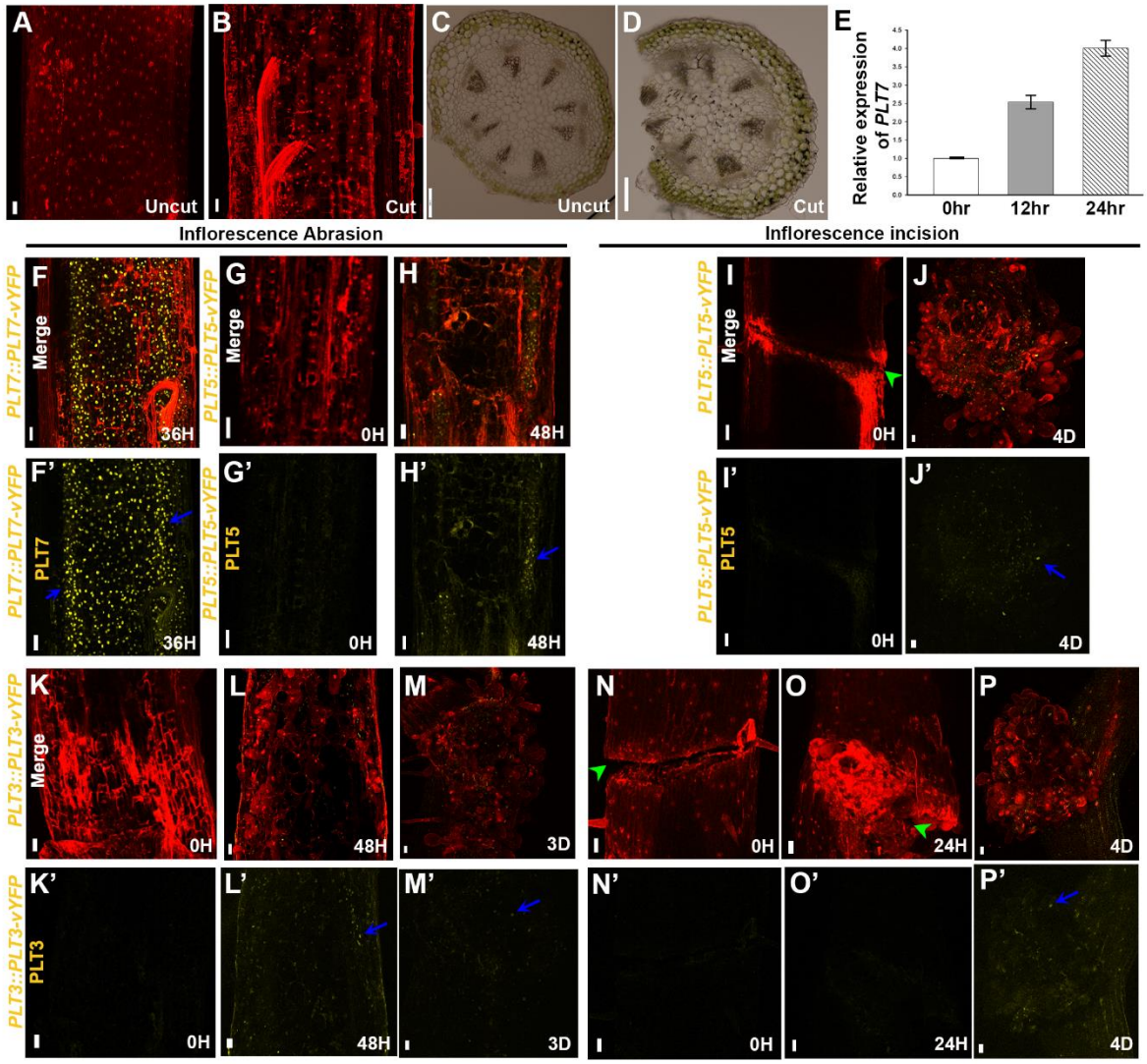

Figure S1: Dynamic expression of PLT in response to inflorescence injury Inflorescence stem abrasion causes damage to epidermal and vascular tissues: (A, C) Undamaged inflorescence stem. (B, D) Sections revealing damaged epidermis and sub-epidermal layers including vascular tissue post inflorescence abrasion. A and B represent longitudinal sections. C and D represent transverse sections. Red colour in A, B is propidium iodide staining.

PLT7 transcript level in wildtype upon partial inflorescence incision: (E) Injured inflorescence segment encompassing the narrow domain on either side of partial slit were collected at 0 h, 12 h and 24 h from growing inflorescence stem. Expression levels are normalized to ACTIN2. Error bar represents s.e.m. from three independent biological replicates.

PLT show dynamic expression in growing aerial organs during wound healing: (F, F') Expression of *PLT7::PLT7-vYFP* in response to inflorescence abrasion. Note the expression of *PLT7::PLT7-vYFP* in sub-epidermal tissues and near vascular tissue (blue arrow). (G-J') Expression of *PLT5::PLT5-vYFP* during natural regeneration. Response to inflorescence abrasion (G-H') and inflorescence partial incision (green arrowhead) (I-J'). Note the increase in expression of *PLT5::PLT5-vYFP* in wounded vascular tissue in H' (blue arrow). (J') Weak expression of *PLT5::PLT5-vYFP* in callus formed in response to injury. (K-P') Expression of *PLT3::PLT3-vYFP* during natural regeneration. Response to inflorescence abrasion (K-M') and inflorescence partial incision (N-P'). Weak expression of *PLT3::PLT3-vYFP* is observed in sub-epidermal tissues (L') and in the callus formed in response to wounding (M' and P').

(F'-J' and K'-P'): maximum intensity projection of Z stack in YFP channel corresponding to (F-J and K-P). Red colour represents propidium iodide staining. Green arrowheads: partial inflorescence incision. Blue arrows: Expression of *PLT3, PLT5, PLT7* in response to wounding. Scale bar: 50 µm except in C and D where scale bars represent 1mm. Brightness of YFP channel has been increased in H', J', L', M' and P' for visibility. The panels (F-P) represent different samples at each time point.

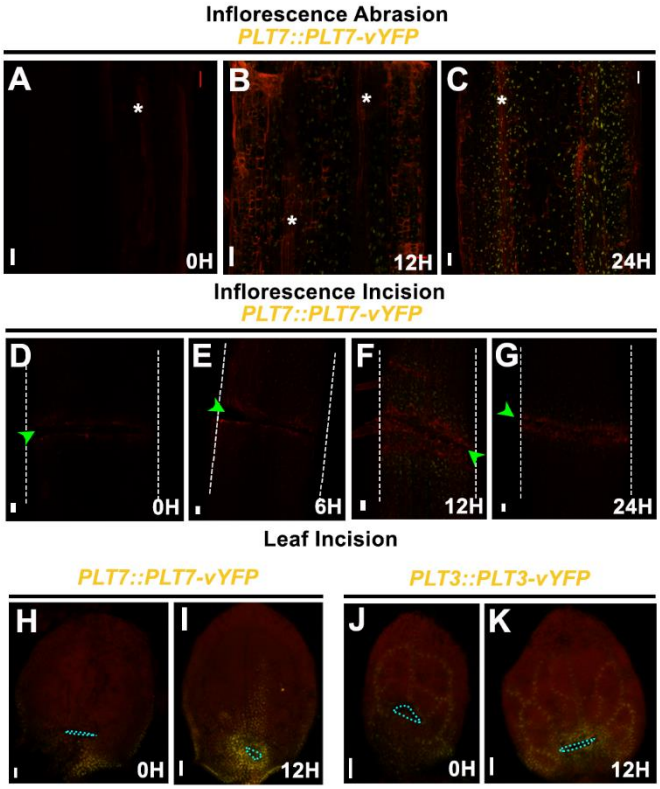

Figure S2: *PLT3, PLT5* and *PLT7* genes are locally induced after mechanical injury

(A-G) *PLT7::PLT7-vYFP* expression (yellow) post abrasion (A-C) and partial incision (green arrowhead) (D-G) in growing inflorescence. White asterisks: vascular tissues exposed by damage to epidermal and sub-epidermal layers following local abrasion. White dashed line: Inflorescence outline. (H-K) Upregulation of *PLT7::PLT7-vYFP* (H,I) and *PLT3::PLT3-vYFP* (J,K) (yellow) near wound site following leaf incision (blue dotted area: incision site). The panels represent average intensity projections of merged panels in Fig. 1 and each panel represent different samples at each time point. Red signal is propidium iodide staining in (A-G) and chlorophyll autofluoroscence in (H-K). Scale bars:50µm.

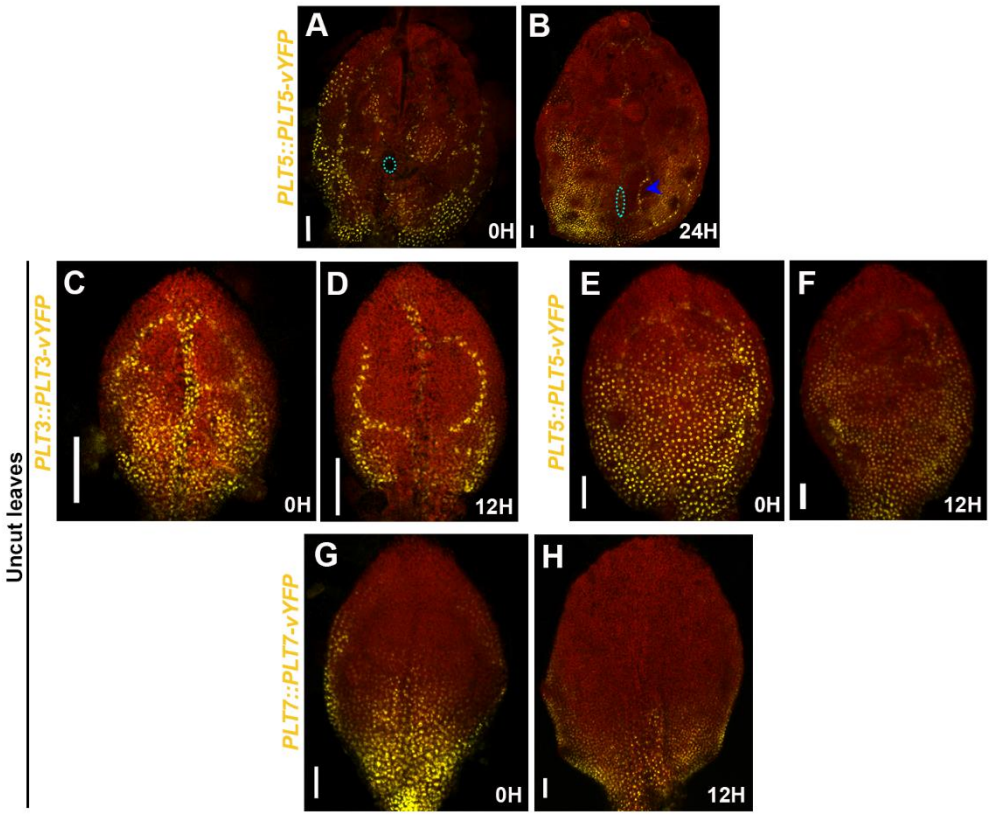

Figure S3: PLT expression in undamaged and injured leaves

(A, B) *PLT5::PLT5-vYFP* expression in adjacent vascular strand (blue arrowhead) post incision (B). (C-H) Expression of *PLT3::PLT3-vYFP*(C, D), *PLT5::PLT5-vYFP* (E, F), *PLT7::PLT7-vYFP* (G, H), in wildtype undamaged leaves.

Red colour represents chlorophyll autofluorescence. B represents a subset of Z stack. Brightness and contrast have been adjusted in propidium iodide channels for clarity of cut part. Blue dotted area: site of incision. Scale bars: 50µm.

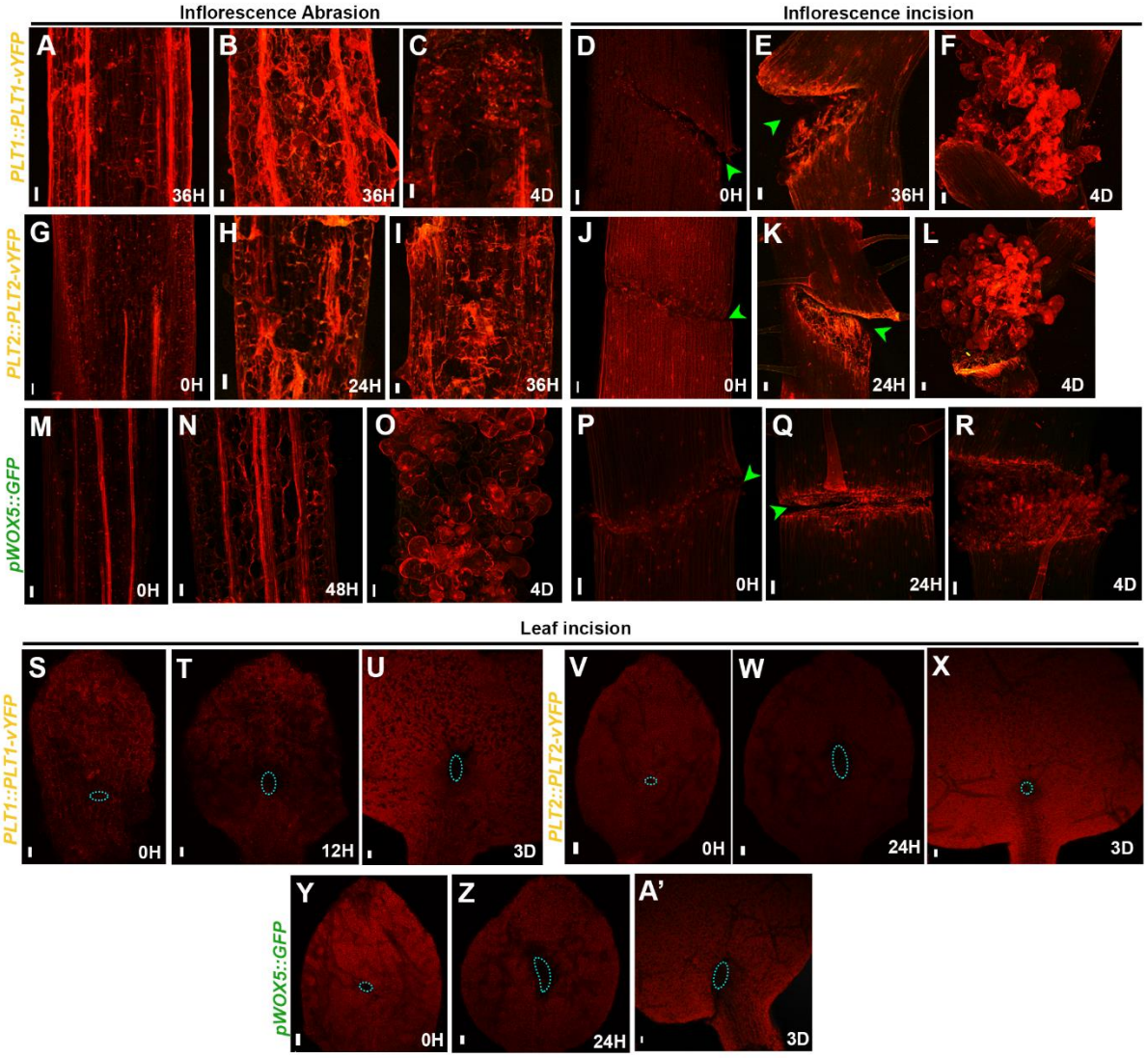

Figure S4: Absence of root stem cell regulators during wound repair in aerial organs

(A-A') Absence of *PLT1::PLT1-vYFP* (A-F, S-U), *PLT2::PLT2-vYFP* (G-L, V-X) and *pWOX5::GFP* (M-R, Y-A') following injury in growing aerial organs. Red colour in (S-A') represent autofluorescence and propidium iodide staining in the rest. Green arrowheads: partial incision in inflorescence. Blue dotted area: incision site. Scale bars: 50µm. Brightness and contrast have been adjusted in propidium iodide channels for clarity.

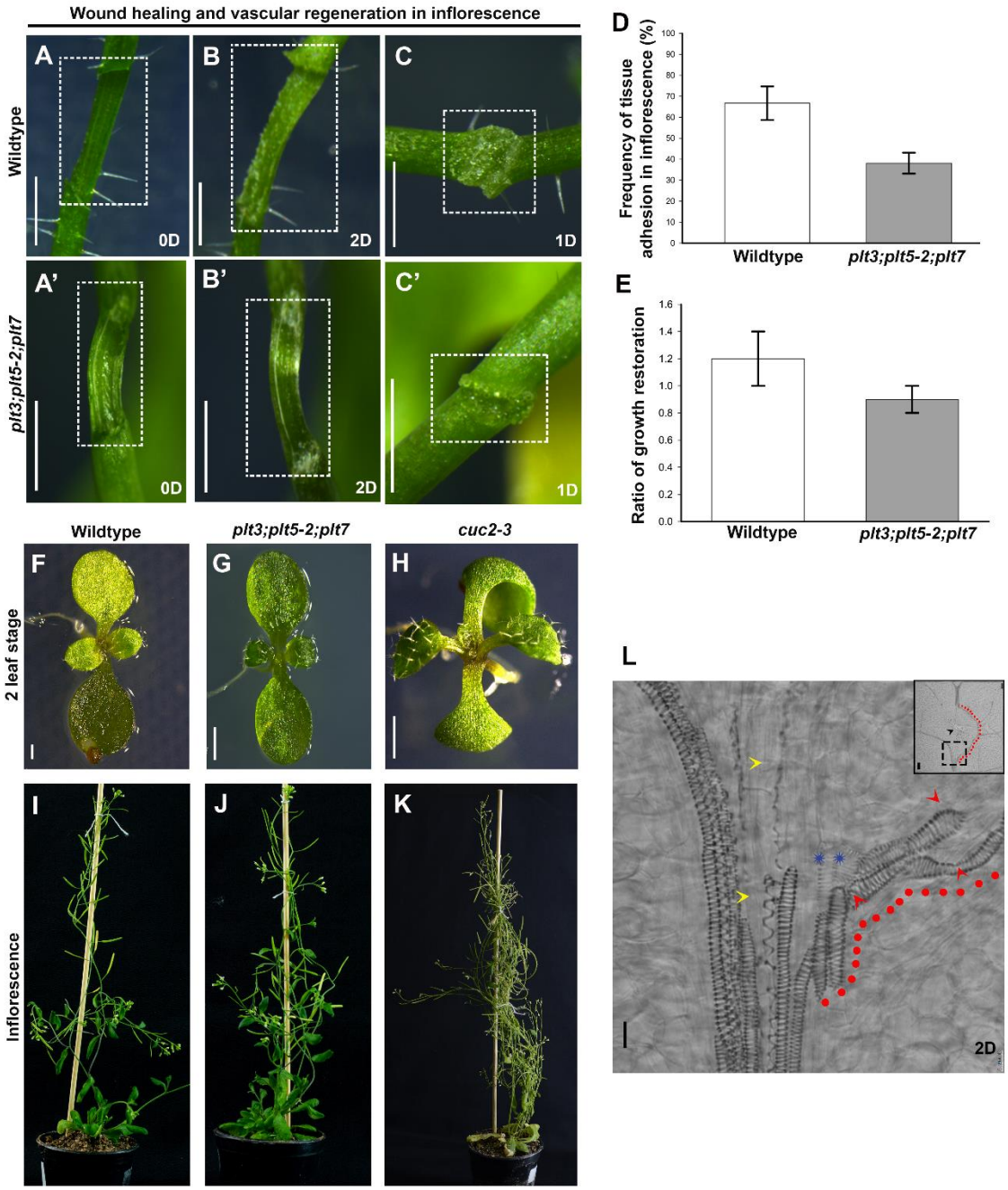

Figure S5: PLT activate innate regenerative responses to injuries in aerial organs growing in normal developmental context

(A, A') Inflorescence abrasion in wildtype (A) and *plt3;plt5-2;plt7* (B). (B,B') Wildtype inflorescence stem with cell proliferation (B) while *plt3;plt5-2;plt7* (B') inflorescence stem failed to show any proliferation.(C, C', D) More callus formation in wildtype (C) 24 h following inflorescence incision leading to increased frequency of tissue adhesion (D) in wildtype as compared to *plt3;plt5-2;plt7* (C'). Dotted rectangle: area of inflorescence damage. (E) Graph representing growth restoration in wildtype and *plt3;plt5-2;plt7* post partial incision in inflorescence.

(F-K) Mutants do not display defect in the normal growth of leaves and inflorescence stem as compared to wildtype.

(L) Zoomed in image shows lower cut end of midvein, two days post leaf incision. Yellow arrowheads mark degenerating vascular strands at lower cut end of midvein. Blue star: initiation of procambium differentiation into vascular cells. Red arrowheads: differentiated xylem vessel elements formed in response to injury. Red dots indicate regenerating vascular stand. Inset shows zoomed out image with black arrow marking site of leaf incision. Area in inset enclosed in dashed line is enlarged in (L).

Scale bar:1mm in all panels except L (Scale bar: 50μm)

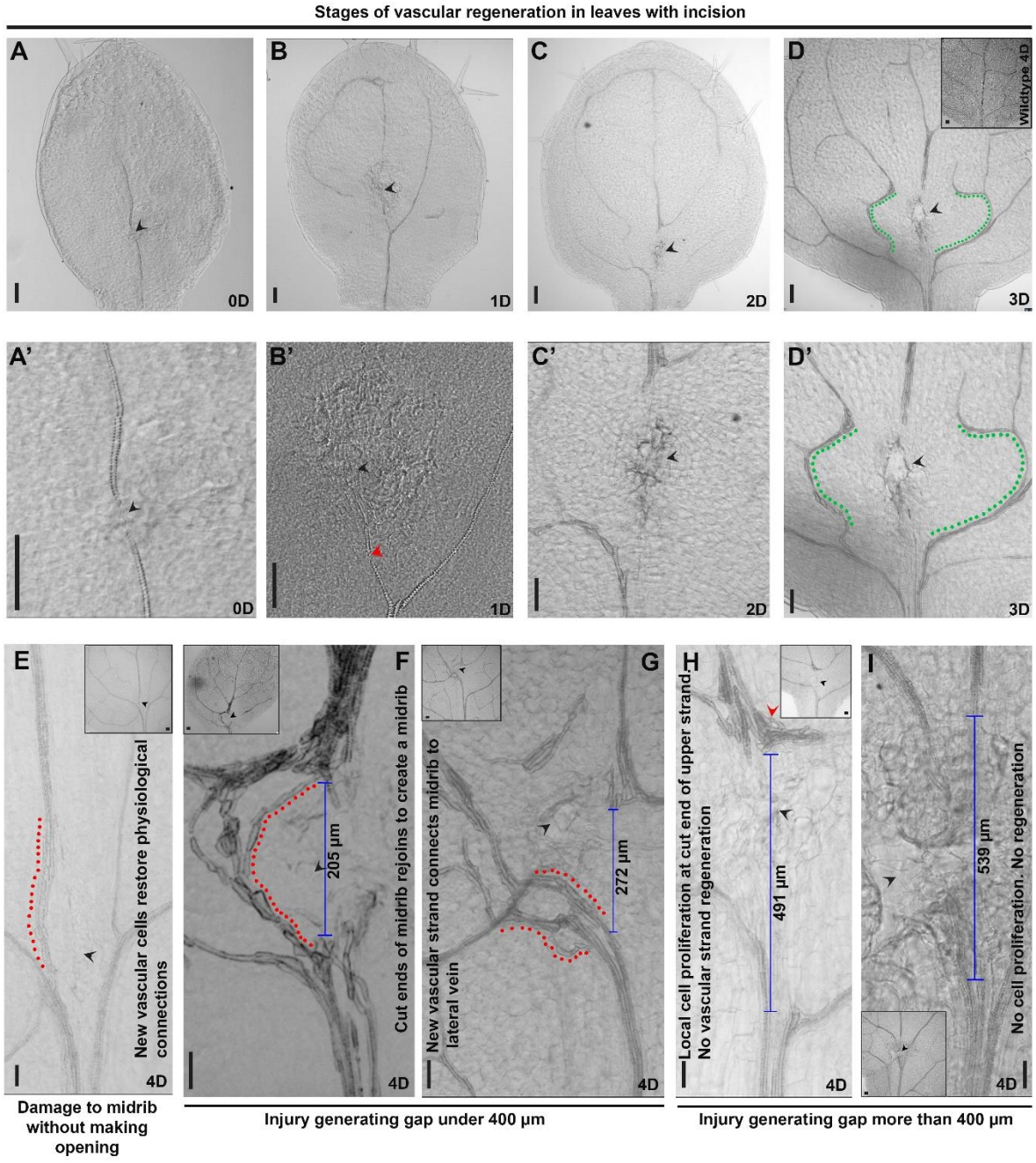

Figure S6: Response to midvein injury in leaf is dependent on the extent of tissue damage

(A-D') Stages of vascular regeneration in wildtype leaves with incision: (A, A') Incision (black arrow) in midvein of 5 dpg old wildtype leaf. Note that only midvein is differentiated at this stage. (B,B') Wildtype leaf- with incision on midvein 1 day post injury. Red arrow head: degenerating vascular strand. (C,C') Wildtype leaf with incision on midvein 2 day post injury. (D, D') Wildtype leaf with incision on the midvein 3 days post injury. New vascular cells form between lateral veins creating a venation pattern (green dots) which does not occur in uninjured wildtype leaf (inset). (A'-D') Zoomed

in images of panels corresponding to (A-D).

(E-I) Responses to midvein injury in growing leaf. (E) Regeneration of new vascular cells (red dotted line) restore physiological connection in midvein when incision does not create an opening in the leaf. (F) Regenerating vascular strands (red dotted lines) rejoins disconnected ends of midvein by creating a D shaped loop (G) Regenerating vascular strands rejoins lower cut end of midvein to lateral vein. (H) Local cell proliferation (red arrow) at the cut end of upper strand but no regeneration of vascular strands. (I) No vascular cell proliferation or regeneration due to extensive area of damage creating opening in the leaf. Insets: Zoomed out images showing site of incision. Black arrowheads: Site of incision.

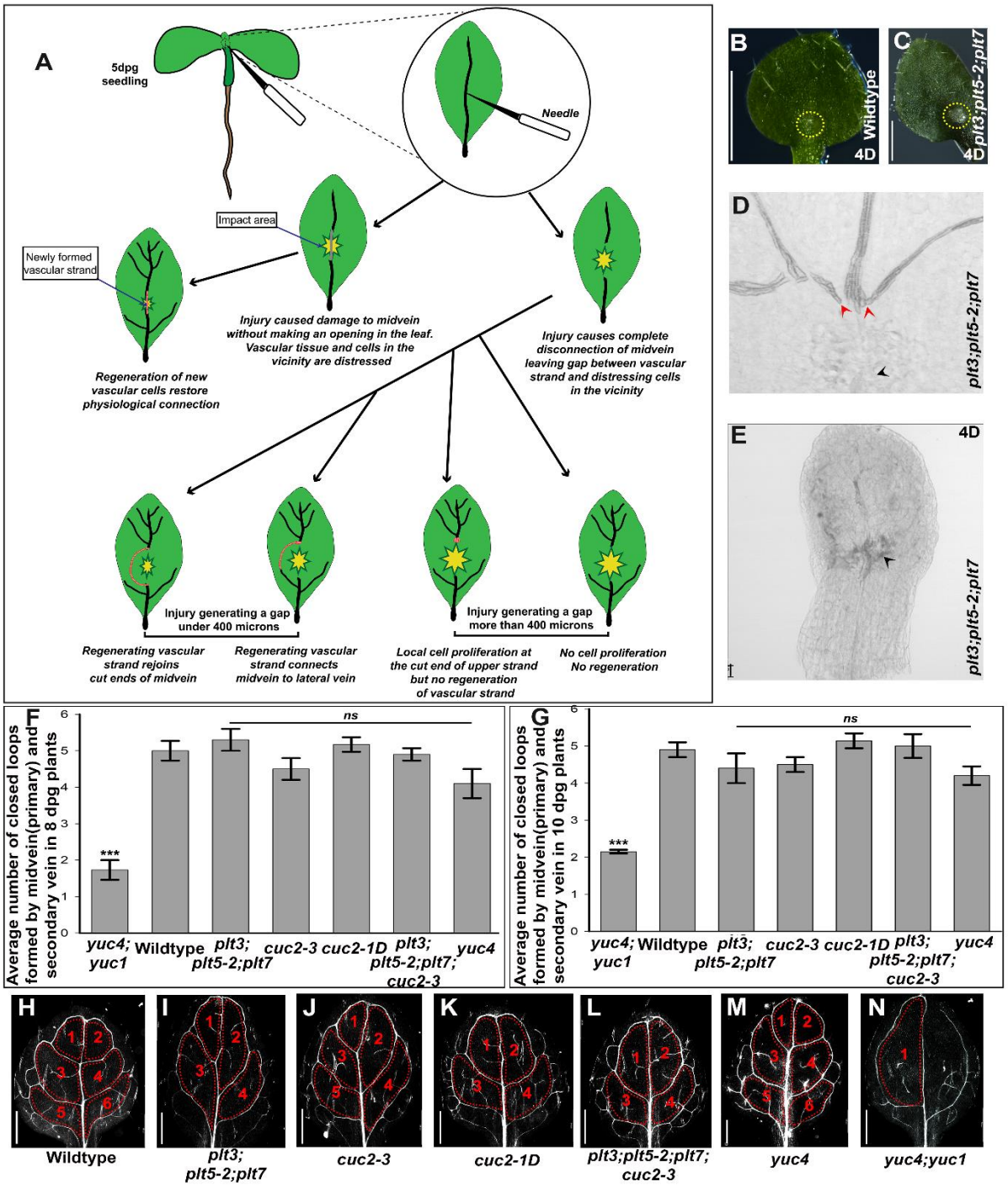

Figure S7: Normal development of vein loops in wildtype and mutants

(A) Schematic representation showing vascular regeneration in response to injuries of varying sizes in the midvein of growing leaf.

(B-D) Proliferation in epidermis (C) and vascular strand (D) (red arrowhead) of *plt3;plt5-2;plt7* leaf following leaf incision (site of incision marked by yellow dotted circle/ black arrowhead). No local cell proliferation was observed on wildtype leaf surface (B).

(E) Following incision many of the *plt3;plt5-2;plt7* mutant leaves display stunted growth and development. Black arrowhead: site of incision.

(F, G) Number of vein loops formed by primary and secondary vein showing continuity of formation of midvein and lateral veins during normal development of first pair of wildtype and mutant leaves (collected from 8dpg and 10 dpg plants). (8dpg samples: p value: *plt3;plt5-2;plt7=0.7; cuc2-3=0.3; cuc2-1=0.6; plt3;plt5-2;plt7;cuc2-3=0.8; yuc4=0.06; yuc4;yuc1=2x10*$^{-16}$) (10dpg samples: p value: *plt3;plt5-2;plt7=0.2; cuc2-3=0.3; cuc2-1=0.5; plt3;plt5-2;plt7;cuc2-3=0.8; yuc4=0.35; yuc4;yuc1=3.5x10*$^{-14}$ *).*

(H-N) Venation pattern in leaves of wildtype and mutants: Mutants (except negative control-*yuc4;yuc1*) does not show significant change in formation of closed vein loops as compared to wildtype leaves. Red dotted lines and numbers mark closed vein loops formed by primary vein (midvein) and secondary vein (lateral vein).

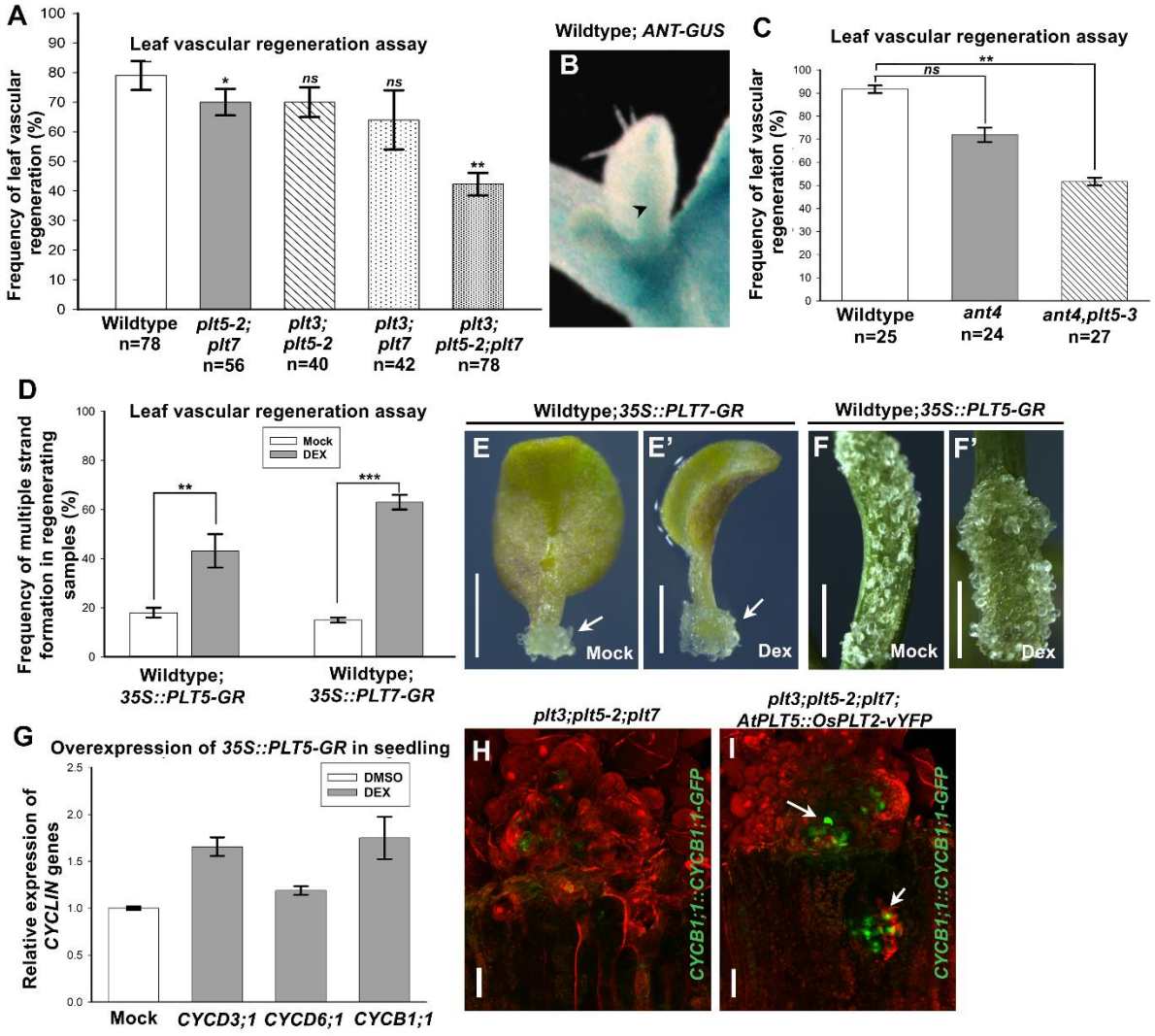

Figure S8: PLT5 and PLT7 are sufficient to promote multiple strand formation and wound repair.

(A) Frequency of leaf vascular regeneration in wildtype, *plt* double mutants and *plt3;plt5-2;plt7* triple

mutants.(*p=0.025;**p=0.008;ns,p>0.05)

(B) Expression of *AINTEGUMENTA* in leaf vasculature (black arrow).

(C) Frequency of leaf vascular regeneration in wildtype, *ant4* mutant and *ant4,plt5-3* double mutant(ns, p>0.05;**p=0.004)

(D) Increased multiple strand formation upon overexpression of *35S::PLT5-GR* and *35S::PLT-GR* during vascular regeneration in response to midvein incision. (E, E') Increased callus formation (white arrow) from cut end of leaf on ectopic induction of *35S::PLT7-GR* (E') as compared to control (E). (F, F') Increased callus formation on the surface of inflorescence stem following abrasion and induction of *35S::PLT5-GR* (F') as compared to control (F) (**p=0.007; ***p=1.2x10^{-5}).

(G) Expression of *CYCLIN* genes in response to overexpression of *35S::PLT5-GR* in growing seedlings. Expression levels are normalized to ACTIN2. Error bar represents s.e.m. from three independent biological replicates.

(H,I) *plt3;plt5-2;plt7*(H) barely shows any cell proliferation marked by cell cycle progression marker *CYCB1;1::CYCB1;1-GFP* as compared to strong expression detected in clusters (white arrow) of actively dividing cells forming callus in response to inflorescence abrasion in *plt3;plt5-2;plt7;AtPLT5::OsPLT2-vYFP* (I). Confocal imaging was performed only for GFP excitation and emission detection.

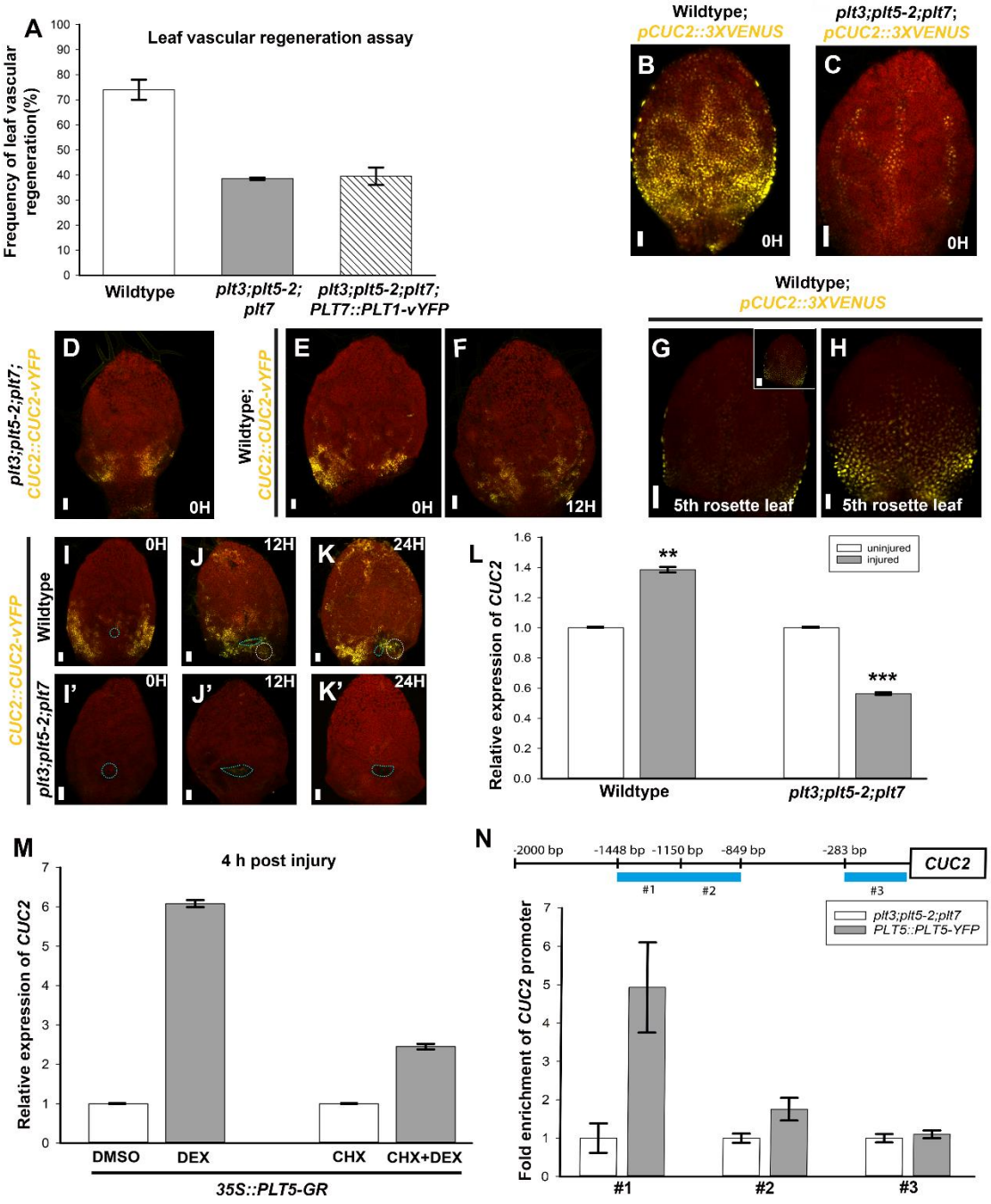

Figure S9: PLT directly activates CUC2 during wound response

(A) Leaf vascular regeneration in wildtype, *plt3;plt5-2;,plt7* and *plt3;plt5-2;plt7;PLT7::PLT1-vYFP*

(B- H) Expression of *CUC2* in undamaged leaves. Expression of *pCUC2::3XVENUS* (B, C) and *CUC2::CUC2-vYFP* (D-F) in undamaged leaves. (G) Single optical section showing expression of *pCUC2::3XVENUS* in the leaf margin of fifth rosette leaf. Inset in (G) represent stacked image of the same leaf. (H) *pCUC2::3XVENUS* expression is absent from the hydathode and higher in the leaf sinus as reported previously (Nikovics *et al.*, 2006; Bilsborough *et al.*, 2011). Except (G) and (H) (5th rosette leaves), all other panels present leaves belonging to 1st pair of rosette leaves.

(I,I') *plt3;plt5-2;plt7* shows reduced expression of *CUC2::CUC2-vYFP* as compared to wildtype.
(J-K') Upon incision wildtype shows expanded domain of expression of *CUC2::CUC2-vYFP* unlike *plt3;plt5-2;plt7*. White dotted circle marks upregulation of YFP expression near wounded area. Blue dotted line marks incision.
(L) Upregulation of *CUC2* transcript in injured wildtype leaf at 12 h post injury as compared to control uninjured wildtype leaves. Downregulation of *CUC2* transcript in injured *plt3;plt5-2;plt7* leaves as compared to control uninjured *plt3;plt5-2;plt7* leaves. (**p=0.002;***p=0.0004)
(M) Transcript level of *CUC2* upon induction of PLT5 with DEX treatment and with cycloheximide treatment.
Expression levels in (L) and (M) are normalized to ACTIN2. Error bar represents s.e.m. from three independent biological replicates
(N) ChIP-qPCR Analysis: ChIP-qPCR experiment in callus tissues shows direct binding of PLT5 fusion protein to the *CUC2* promoter. The results are shown as fold enrichment relative to *plt3;plt5-2;plt7* loss of function mutant. A strong binding of PLT5 is noticed at the fragment #1 (-1150 to -1448 bp) followed by a weak binding at #2 (-849 to -1149 bp) and no significant binding at the fragment #3 (-1 to -283 bp) of the upstream sequence of *CUC2*. Error bars show the standard error of the ChIP-qPCR reactions performed in triplicates.

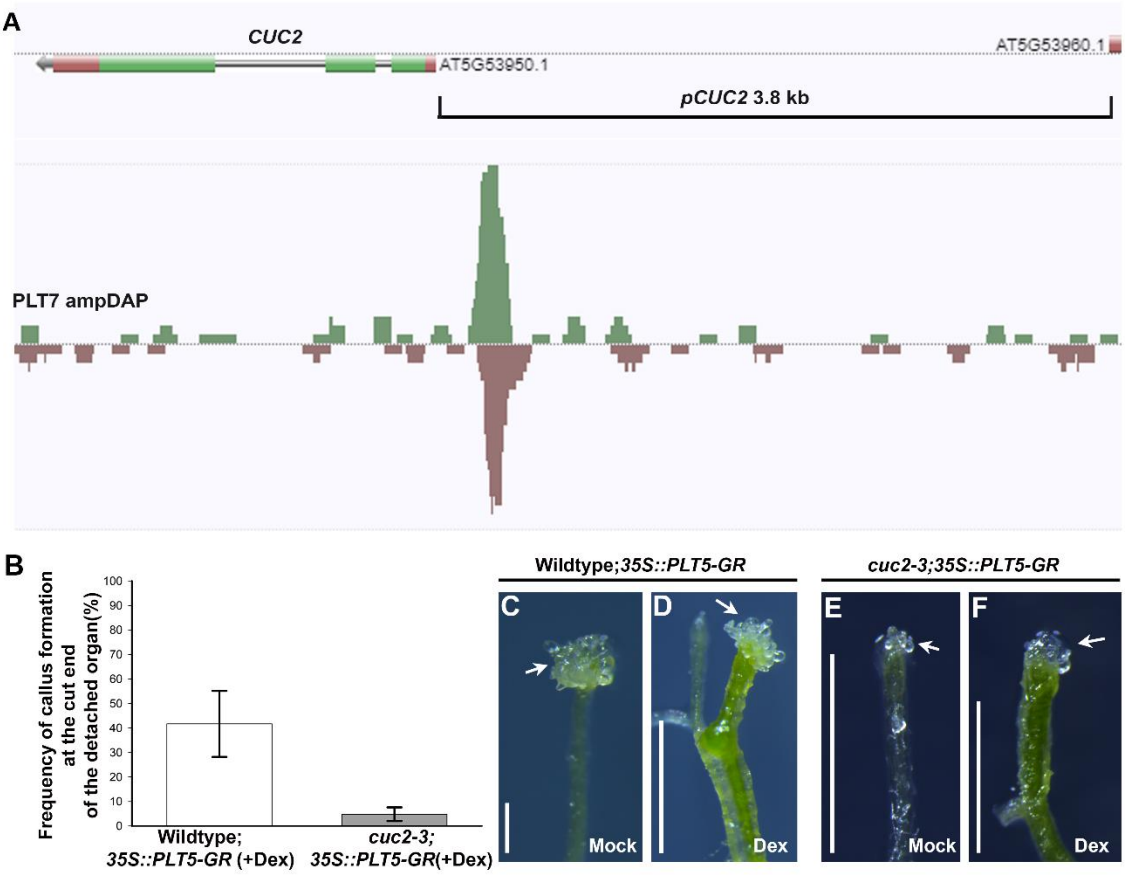

Figure S10: PLT acts through CUC2 during wound repair

(A) PLT7 binds the *CUC2* promoter (neomorph.salk.edu). Indicated region shows *pCUC2*, which was used in the luciferase reporter assay.

(B) Frequency refers to the number of excised organs showing callus formation at the cut end. In addition to frequency, the extent of callus formation was also reduced in *cuc2-3;35S::PLT5-GR.*

(C, D) Wildtype;*35S::PLT5-GR* upon continuous DEX induction (n=12/15) (D) following excision shows increased extent of callus formation unlike in mock treated control (n=9/10) (C) at the detached end of root.

(E, F) *cuc2-3;35S::PLT5-GR* upon continuous DEX induction (n=15/20) (F) following excision shows no increase in extent of callus formation as compared to mock treated control (n=16/20) (E) at the detached end of root.

Arrow: Callus formation. Scalebars:1mm.

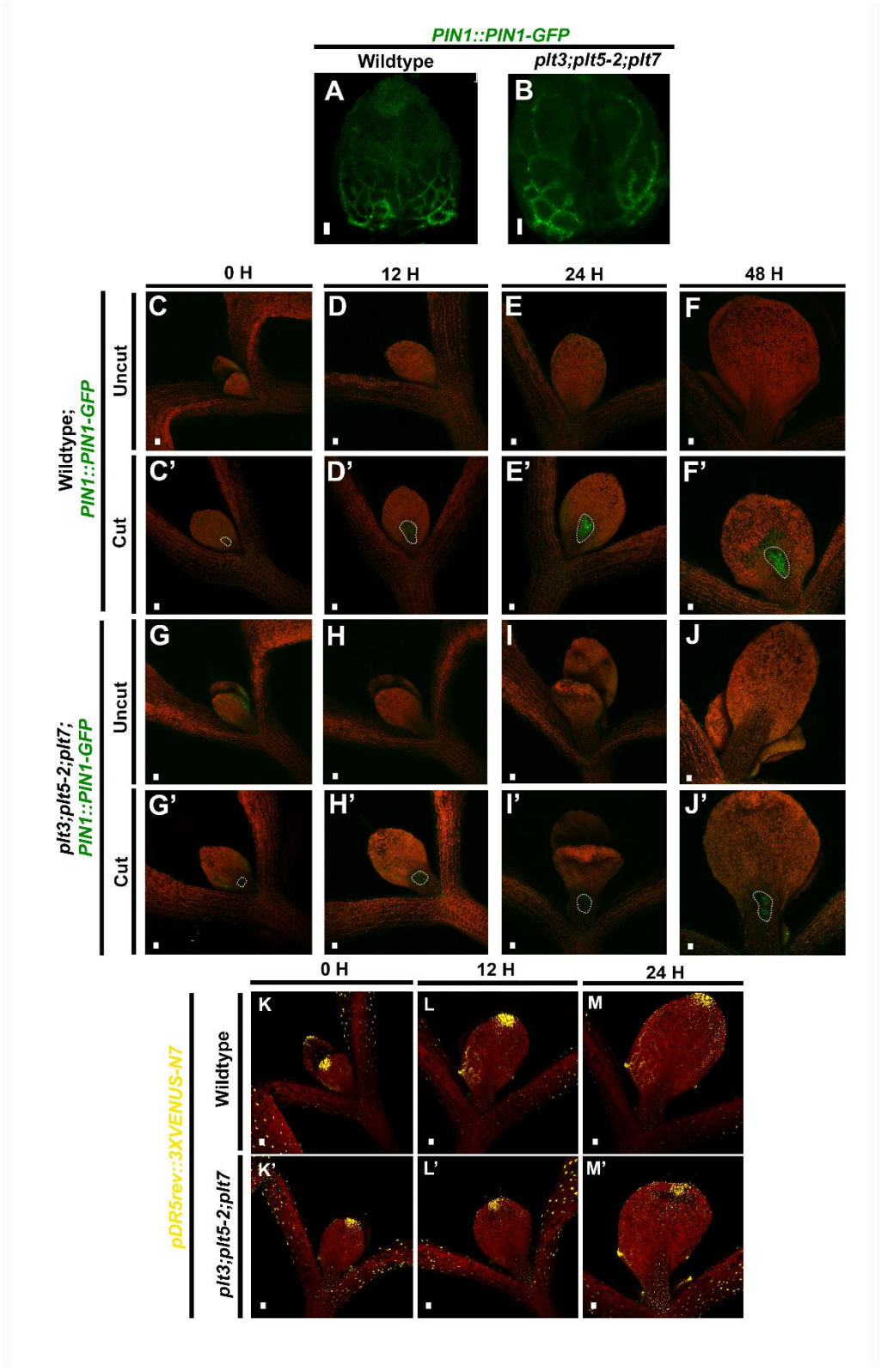

Figure 11: PIN1 expression and auxin response are not defective in *plt* mutant during normal development

(A, B) *PIN1::PIN1-GFP* expression in undamaged leaves of wildtype (A) and *plt3;plt5-2;plt7* (B). PIN1 expression is visible in the basal part of the leaves in both wildtype and *plt3;plt5-2;plt7*.

(C-J') Time lapse images showing expression of *PIN1::PIN1-GFP* in wildtype (C-F') and *plt3;plt5-2;plt7* (G-J'). (C-F) and (G-J) represent uninjured leaves while the remaining represent injured leaves in which injured areas are marked by white dotted lines.

(K-M') Timelapse images showing expression of *pDR5rev::3XVENUS-N7* in wildtype (K-M) and p*lt3;plt5-2;plt7* (K'-M') uninjured leaves.

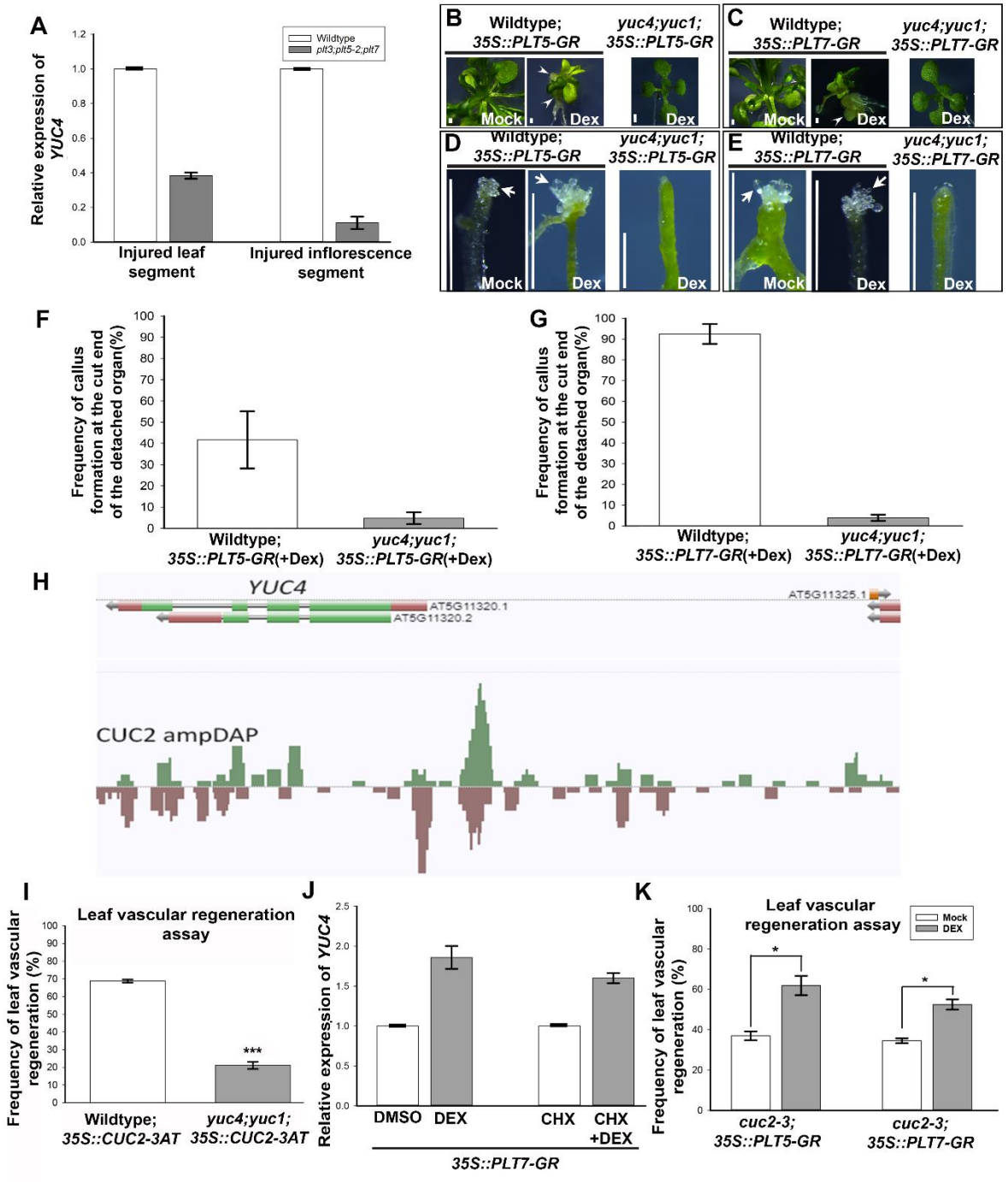

Figure S12: PLT acts though YUC4 during reprogramming and wound repair

(A)*YUC4* transcript level in injured leaf segments and in injured inflorescence segments of wildtype and *plt3;plt5-2;plt7* mutant. Expression levels in A is normalized to ACTIN2. Error bar represents s.e.m. from three independent biological replicates.

(B) Growing seedlings of Wildtype*;35S::PLT5-GR* upon DEX induction shows callus formation (arrowheads) from shoot and root leading to stunted growth of the plant, unlike mock treated control, which does not show any ectopic phenotypes. However *yuc4;yuc1;35S::PLT5-GR* does not show any cellular reprogramming even upon DEX induction.

(C) Growing seedlings of Wildtype*; 35S::PLT7-GR* upon DEX induction shows callus formation (arrowhead) from hypocotyl and root leading to stunted growth of the plant, unlike mock treated control, which does not show any ectopic phenotypes. However *yuc4;yuc1;35S::PLT7-GR* does not show any cellular reprogramming even upon DEX induction.

(D) Wildtype;*35S::PLT5-GR* upon DEX induction (n=15/20) shows increased extent of callus formation unlike in mock treated control of detached organ (n=10/13). However *yuc4;yuc1;35S::PLT5-GR* (n=20/20) shows barely any callus formation upon DEX induction.

(E) Wildtype;*35S::PLT7-GR* upon DEX induction (n=9/10) shows increased extent of callus formation unlike in mock treated control of detached organ (n=7/11). However *yuc4;yuc1;35S::PLT7-GR* (n=14/15) rarely shows callus formation upon DEX induction.

(F,G) Frequency refers to the number of excised organs showing callus formation at the cut end. In addition to frequency, the extent of callus formation at the wounded end of detached organ was extremely reduced in *yuc4;yuc1* as compared to wildt ype upon DEX induction of *35S::PLT5-GR* (F) and *35S::PLT7-GR* (G)

(H) CUC2 binds the *YUC4* promoter as shown by DAP-seq analysis (neomorph.salk.edu).

(I)Frequency of leaf vascular regeneration in Widtype;*35S::CUC2-3AT* and *yuc4,yuc1;35S::CUC2-3AT* (***$p=2x10^{-6}$).

(J) Transcript level of *YUC4* upon induction of *35S::PLT7-GR* with DEX treatment and with cycloheximide treatment at 4 h post injury. Expression levels are normalized to ACTIN2. Error bar represents s.e.m. from three independent biological replicates.

(K) Frequency of leaf vascular regeneration upon overexpression of *35S::PLT5-GR* and *35S::PLT7-GR* in *cuc2-3* mutant.

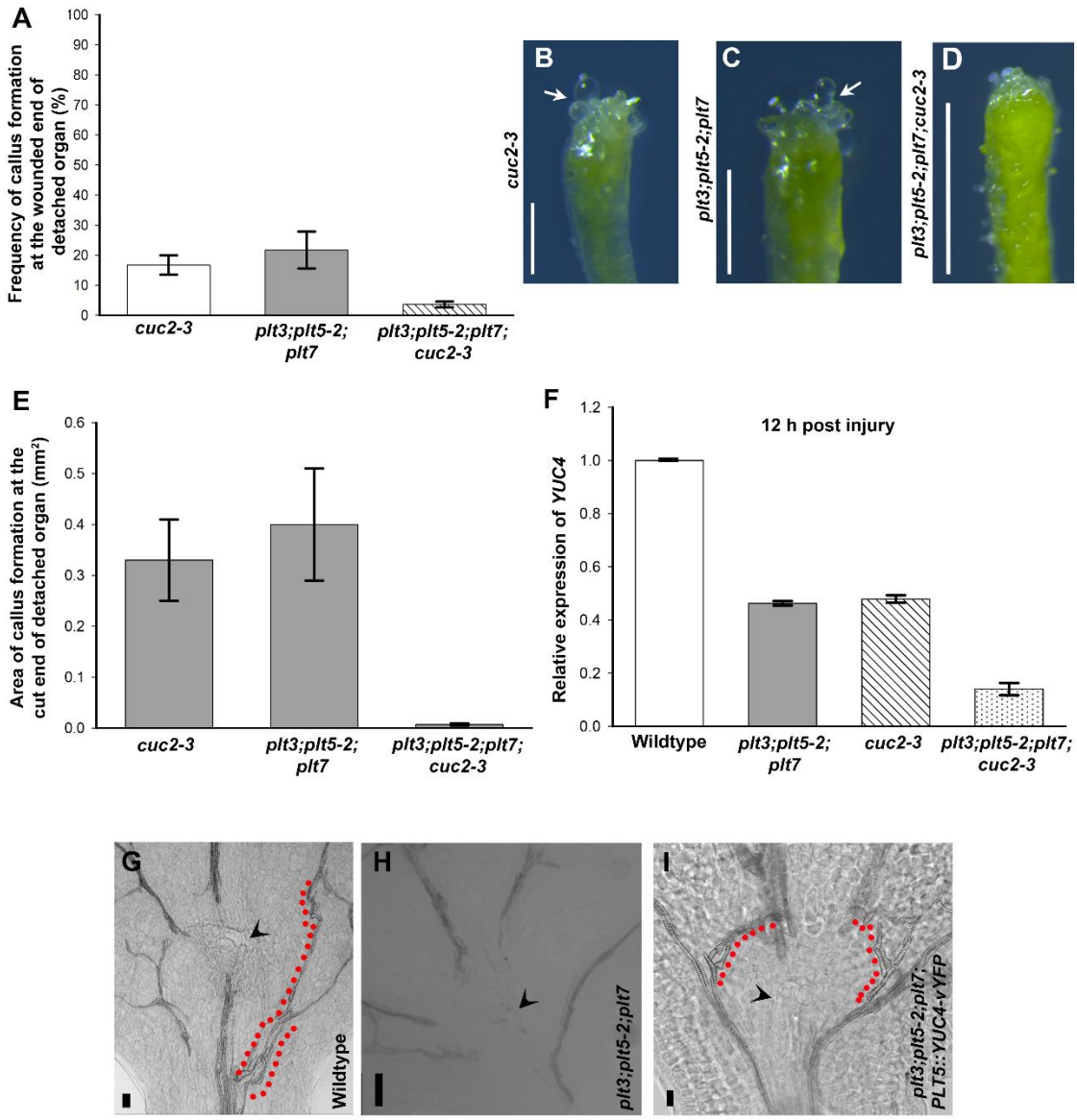

Figure 13: PLT and CUC2 regulate *YUC4* in a coherent feed forward loop

(A) Frequency refers to the number of excised organs showing callus formation at the cut end.

(B-D) In addition to frequency, extent of callus formation (white arrow) was drastically reduced in *plt3;plt5-2;plt7;cuc2-3* as compared to *cuc2-3* and *plt3;plt5-2;plt7* which showed moderate callus formation at the cut ends of detached organs.

(E) Area of callus formation at the cut end of detached organs of *cuc2-3, plt3;plt5-2;plt7* and *plt3;plt5-2;plt7;cuc2-3*.

(F) Relative expression levels of *YUC4* in wildtype and mutants. Expression levels are normalized to ACTIN2. Error bar represents s.e.m. from three independent biological replicates.

(G-I) Vascular strand regeneration assay in wildtype (G), *plt3;plt5-2;plt7* (H) and *plt3;plt5-2;plt7;PLT5::YUC4-vYFP* (I). Vascular strands fail to regenerate in *plt3;plt5-2;plt7* (H). Black arrowhead marks site of leaf incision. Red dotted lines mark regenerated vascular strands.

Table S1: Synergistic interaction between PLT and CUC2 during vascular regeneration

Genotype	Frequency of leaf vascular regeneration (%)
plt3^{+}*/-;plt5-2*$^{+}$*/-;plt7*$^{+}$*/-*	70.52
cuc2-3^{+}*/-*	71.66
plt3^{+}*/-;plt5-2*$^{+}$*/-;plt7*$^{+}$*/-;cuc2-3*$^{+}$*/-*	36.80

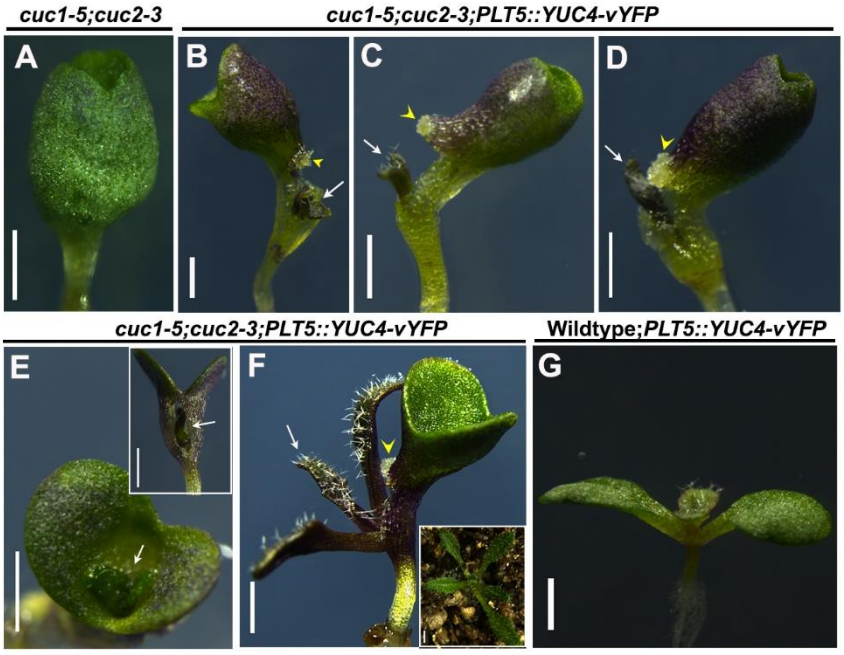

Figure S14: YUC4 rescued post embryonic development in *cuc1-5;cuc2-3* mutant

(A) Cup shaped cotyledon in *cuc1-5,cuc2-3* mutant (none out of 80 cup shaped plants produced shoot). (B-F) Reconstitution of local auxin biosynthesis gene in PLT5 domain rescues post embryonic development, giving rise to fully developed leaves (marked by white arrows). Out of 48 plants with cup shaped cotyledon, 20 produced shoot from base of cotyledon. Callus formed at the base of cotyledon caused by the emergence of the shoot is marked by yellow arrowheads. (G) Wildtype;*PLT5::YUC4-vYFP* showing normal shoot formation.

SUPPLEMENTARY INFORMATION

MATERIALS AND METHODS

Plasmid construction

The transcriptional fusion constructs of *pWUS::3XVENUS-tWUS* was generated by fusing 5.744kb upstream regulatory sequences of *WUS* with *3XVENUS* and 1.635kb of *WUS* 3'UTR. To generate *PLT5::YUC4:vYFP* construct, 5.6kb upstream regulatory elements of *PLT5* and 1.93kb *YUC4* gene

were separately amplified from and incorporated with v*YFP*. *plt3; plt5-2;plt7*, *cuc1-5(-/-);cuc2-3(+/-)* and *cuc2-1D* mutant plants were transformed using the construct. Similarly 1.7kb upstream regulatory element and 4.236kb *ATHB8* gene was incorporated with *vYFP* to generate the translational fusion construct *ATHB8::ATHB8-vYFP*. This construct was co-transformed with PIN1::PIN1-GFP into both wildtype and *plt3;plt5-2;plt7* mutant to generate the double marker transgenic line. *OsPLT2 (LOC_Os06g44750.1)* was cloned under upstream regulatory elements of Arabidopsis PLT5 gene and tagged with vYFP. This construct was transformed into *plt3; plt5-2; plt7*.

Decolourisation and tissue clearing for imaging vascular tissues

To visualize regenerating vascular strands, the injured leaf and inflorescence stem were carefully excised from the growing seedling at different time interval post incision using Vannas straight scissors. Before proceeding for decolorization of chlorophyll, a longitudinal cut was made through the excised inflorescence stem using razor blade to expose the regenerating vascular strands of thick inflorescence tissues. Both leaf and inflorescence stem were dehydrated and the chlorophyll was bleached by incubating the sample consecutively in 15%, 50%, 70% and 96% ethanol for 15 minutes each. Finally, the samples were incubated in absolute ethanol for 12 h overnight. The sample was then rehydrated by transferring from 100% ethanol to 96%, 70%, 50% and finally 15% ethanol in the reverse order with 15 minutes incubation in each concentration of ethanol. Then the samples were incubated for 2-3 h in freshly prepared clearing solution consisting of 8 g chloral hydrate (Sigma), 1 ml 100% glycerol (Sigma) and 3 ml distilled water. The cleared samples were mounted on slides using the clearing solution with the adaxial surface of the leaf and the longitudinally cut surface of the inflorescence stem facing upward. Coverslip was placed carefully avoiding any bubble formation and curling of the tissues.

Sample preparation for qRT-PCR

For qRT-PCR, inflorescence abrasion was done in wildtype Columbia plants and *plt3;plt5-2; plt7* triple mutant. The injured part of inflorescence was harvested after four days and used for RNA extraction. Leaves were injured in the context of growing seedling and the entire seedling without the root was taken for qPCR. Likewise, *PLT5*, *PLT7* and *CUC2* were induced using steroid inducible constructs namely, *35S*::*PLT5-GR* , *35S*::*PLT7-GR* and *35S*::*CUC2-GR*. After performing inflorescence abrasion the complete plants were transferred to MS plates containing 20 µM dexamethasone (DEX) followed by flooding the plate with liquid MS medium with DEX. Mock treatment was performed using MS medium supplemented only with

DMSO and flooding was performed using liquid MS supplemented with DMSO. The wounded inflorescence samples were collected at 4 h or 8 h and was used for RNA extraction.

Table S2. Oligonucleotide primers used for cloning and qRT PCR (5'-3')

Primer name	Forward primer	Reverse primer
qRT-PLT5	CTACTCCGGTGGACACTCGT	CGTTCTTCTTCGGAGTAGGC
qRT-PLT7	TTTCCTCGGTGATTCCTTTG	TGACGTGGATCGTAGAATGG
qRT-YUC4	TCCATAATATTAGCGACTGGGTA	CCCTTCTCTCCTTTCCATCC
pCUC2 LUCR	GGGGACAAGTTTGTACAAAAAAGCA GGCTttaattctacattttgtttgg	GGGGACCACTTTGTACAAGAAAG CTGGGTtgttttgaagaagaagataaa
ATHB8 promoter	GGGGACAACTTTGTATAGAAAAGTT GTTCGGATAAACCAATTTTCAAATG	GGGGACTGCTTTTTTGTACAAACT TGTCTTTGATCCTCTCCGATCT
ATHB8 gene	GGGGACAAGTTTGTACAAAAAAGCA GGCTGTATGGGAGGAGGAAGCAATA ATAGTCA	GGGGACCACTTTGTACAAGAAAG CTGGGTTTATAAAAGACCAGTTGA GGAACATGAAGC

Additional primers used in this study have been previously described (Kareem *et al*. 2015)

ChIP-qPCR Analysis.

600 mg fresh weight of five-day-old proliferating callus tissues derived from roots of *PLT::PLT5-vYFP* and *plt3;plt5;plt7* were cross-linked in 1% formaldehyde (Sigma). The isolated chromatin was immunoprecipitated with anti-GFP antibody (5 µl per sample) (Clontech). After several washing steps, the protein–DNA cross-linking was reversed. Further, the DNA was cleaned using PCR Purification Kit (Qiagen).

Table S3. Primers used for ChIP-qPCR

Primer name	Forward primer	Reverse primer
CUC2-ChIP #1	ACATTTTTGGGTGGGAAAT	AGAGAAGATATTTATGCTGCCT
CUC2-ChIP #2	GATTTGCAACCTGTAACTTC	TGTCAGCACAGTACATGATT
CUC2-ChIP #3	TCTTCTCTACGACTTTCTGG	TAAGAAGAAAGATCTAAAGCTTTTG
ACT7-ChIP	CGTTTCGCTTTCCTTAGTGTTAGCT	AGCGAACGGATCTAGAGACTCACCTTG

REFERENCES FOR SUPPLEMENTARY INFORMATION

Bilsborough, G.D., Runions, A., Barkoulas, M., Jenkins, H.W., Hasson, A., Galinha, C., Laufs, P., Hay, A., Prusinkiewicz, P. and Tsiantis, M. (2011). Model for the regulation of Arabidopsis thaliana leaf margin development. *Proc. Natl. Acad. Sci. USA* **108**, 3424-3429. doi: 10.1073/PNAS.1015162108.

Kareem, A., Durgaprasad, K., Sugimoto, K., Du, Y., Pulianmackal, A.J., Trivedi, Z.B., Abhayadev, P.V., Pinon, V., Meyerowitz, E.M., Scheres, B. et al. (2015). PLETHORA genes control regeneration by a two-step mechanism.*Curr. Biol.* **25**, 1017-1030. doi: 10.1016/j.cub.2015.02.022.

Nikovics, K., Blein, T., Peaucelle, A., Ishida, T., Morin, H., Aida, M. and Laufs, P. (2006). The balance between the MIR164A and CUC2 genes controls leaf margin serration in Arabidopsis. *The Plant Cell*. **18**, 2929-2945. doi: 10.1105/TPC.106.045617.